with low <mu> data

W-Ai measurements

Daniil Ponomarenko

10-March-2023

Plan of the talk

- Motivation
- Brief analysis overview
- Updates on MJ estimation

ATLAS Note

ANA-STDM-2020-07-INT1

3rd February 2023

Draft version 0.4

Measurement of angular coefficients in $W \rightarrow \ell\nu$ events in low-μ pp collisions at $\sqrt{s} = 13$ TeV with the ATLAS detector

Link to CDS: https://cds.cern.ch/record/2824052 (last modified 2022-09-30).
Latest version of supporting note is in attachments to the agenda.

Motivation

W mass measurement

$M_W = 80369.5 \pm 6.8\ (\text{stat}) \pm 10.6\ (\text{exp.syst.}) \pm 13.6\ (\text{model.syst.})$ MeV

Limited by data

Experimental: modelling of lepton momentum measurement and hadronic recoil

Theoretical: understanding of vector boson production and decay

Combined categories	Value [MeV]	Stat. Unc.	Muon Unc.	Elec. Unc.	Recoil Unc.	Bckg. Unc.	QCD Unc.	EW Unc.	PDF Unc.	Total Unc.	χ^2/dof of Comb.
m_T-p_T^ℓ, $W^\pm$, e-μ	80369.5	6.8	6.6	6.4	2.9	4.5	8.3	5.5	9.2	18.5	29/27

- Larger source of modelling uncertainty from PDFs
- Total uncertainty on ATLAS W mass measurement ~19MeV still larger than 8MeV from electroweak fit

Why measure Ai in W events?

physics modelling

Data sample	7 TeV, $\mu \sim 9$	
Luminosity	4.5 fb^{-1}	Improuved
Nb. of candidates	$\sim 15 \times 10^6$	
Most sensitive dist.	p_T^ℓ	
Physics Modelling Unc.		
EW	5 → latest MC gen.	2
QCD (p_T^W)	6 → WpT meas.	< 3
QCD (A_i)	6 → data input	< 3
PDFs	9 → PDF profiling	6

- W-Ai analysis (+ x-section):
  - A_i: Stringent test of QCD & physics modelling!
  - X-section measurement as function of the Y.
    - All previous measurements at the LHC are done with lepton η.
  - Charge asymmetry measurement: Input for PDF fits
- Full set of A_i have never been measured before for the W boson!
  - Only A_2 and A_3 were measured by CDF (Phys. Rev. D 73, 052002)

Vector boson production and decay

- Drell Yan $pp \to V \to l\bar{l}$ cross section can be factorised into an **unpolarised** cross-section and **8 angular coefficients** (A_i).

$$\frac{d\sigma}{dp_1 dp_2} = \left[\frac{d\sigma(m)}{dm}\right]\left[\frac{d\sigma(y)}{dy}\right]\left[\frac{d\sigma(p_T, y)}{dp_T dy}\left(\frac{d\sigma(y)}{dy}\right)^{-1}\right]\left[(1+\cos^2\theta) + \sum_{i=0}^{7} A_i(p_T, y) P_i(\cos\theta, \phi)\right]$$

Breit Wigner | Parton shower | Fixed order pQCD

- The angular coefficients:
  - A_0, A_1, A_2 sensitive to vector boson **polarisation**
    - $A_0 - A_2 = 0$ but violated due to higher order QCD effects (e.g. multi-gluon emission..)
  - A_3, A_4 sensitive to **vector and axial couplings** of the boson
    - A_4 directly related to A_{FB}, probes electroweak mixing
  - A_5, A_6, A_7 non-zero only at $\mathcal{O}(\alpha_s^2)$
- QCD production dynamics fully contained in A_i coefficients, while decay kinematics fully contained in coupled angular polynomials

In Collins-Soper frame:

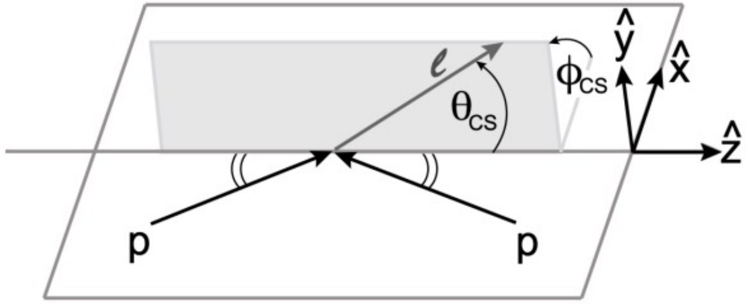

JHEP08(2016)159

Analysis overview

W Ai analysis overview

- Supporting note: ANA-STDM-2020-07-INT1
- Dataset:
  - ATLAS 13 TeV low pileup datasets 335.18 pb^{-1}
  - Statistically limited by small datasets but provides hadronic recoil resolution needed
- Able to measure 1D in p_T^W and separately in y^W
- We focus on the larger coefficients A_0, A_2, A_3, A_4
  - Other coefficients are also get measured, but the analysis is far from having sensitivity to A_5, A_6, A_7
- Channels:
  - $W^- \to e^-\nu, W^+ \to e^+\nu, W^- \to \mu^-\nu, W^+ \to \mu^+\nu$
- Looking forward for EB request

Event selection

Electron	Muon
Tight ID	Medium ID
p_T > 25 GeV	
$\|\eta\|$ < 2.4	
1.37 < $\|\eta\|$ < 1.52	
ptvarcone20/p_T < 0.1	
topoetcone20/p_T < 0.05	
$\|d_0$ sig$\|$ < 5	$\|d_0$ sig$\|$ < 3
$\Delta z_0 \sin\theta$ < 0.5	

- We use signal region selection based on pTW analysis with optimizations for better A_i sensitivity
  - Use same physics objects calibrations
  - + estimate and apply corrections specific for Wai analysis
- Relaxed kinematic cuts:
  - No $E_T^{miss} > 25\ GeV$ cut
  - No $m_T^W > 50\ GeV$ cut
- Use *TightLH* working point for electrons
- Tighter isolation selection:
  - $ptvarcone20/pt$<0.1 && $topoetcone20/pt$<0.05

Analysis

Angular definitions require fully constructed neutrino (will cover in next slides):

- Using Hadronic recoil solve for Neutrino p_z with mass constrain.
- Once the mass constraint is chosen φ_{CS} is solved while the 2 solutions corresponds to a sign ambiguity in $\cos\theta_{CS}$.
- Discovered that adding sign ambiguity only in y^W, not in $\cos\theta_{CS}$ drives our A_4 sensitivity.

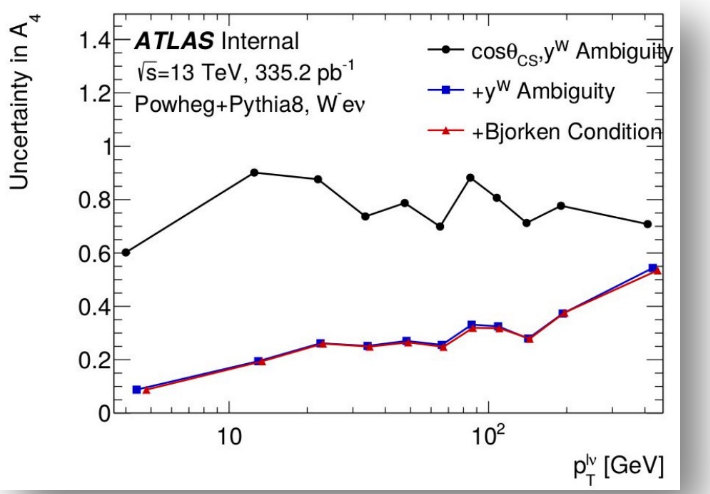

MJ shape estimation follows procedure used by pTW analysis (slides in backup):

- Calculate MJ normalization by linear extrapolation fit for different anti-isolation slices
- Calculate MJ template shape by applying bin-by-bin linear shape extrapolation
- To get MJ shape as a function of |Y| and $p_T^{l,\nu}$ MC samples used: $b\bar{b} + c\bar{c}$ for W→μν channels, JF17 for W→eν channels
- Calorimetric isolation used for e± and track isolation used for μ± channels:
  - Slicing ptvarcone20/pt for W→μν: 8 slicing bins from 0.1 to 0.5
  - Slicing in topoetcone20/pt for W→eν: 8 slicing bins from 0.05 to 0.45

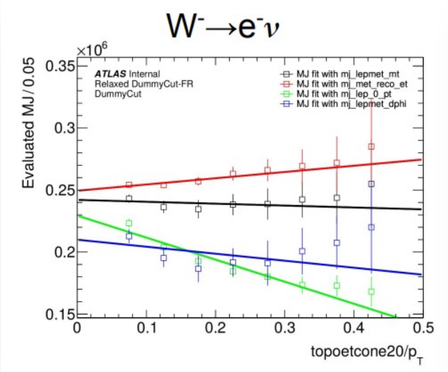

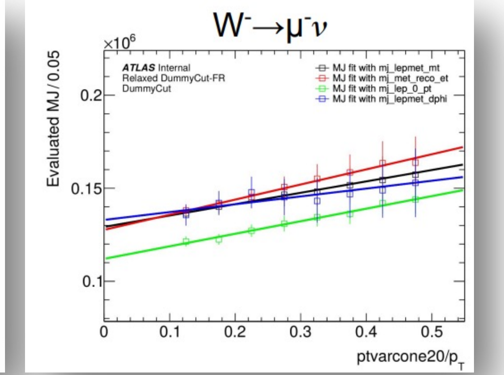

Control plots in the Signal Region for $W^{-} \rightarrow e^{-}\nu$

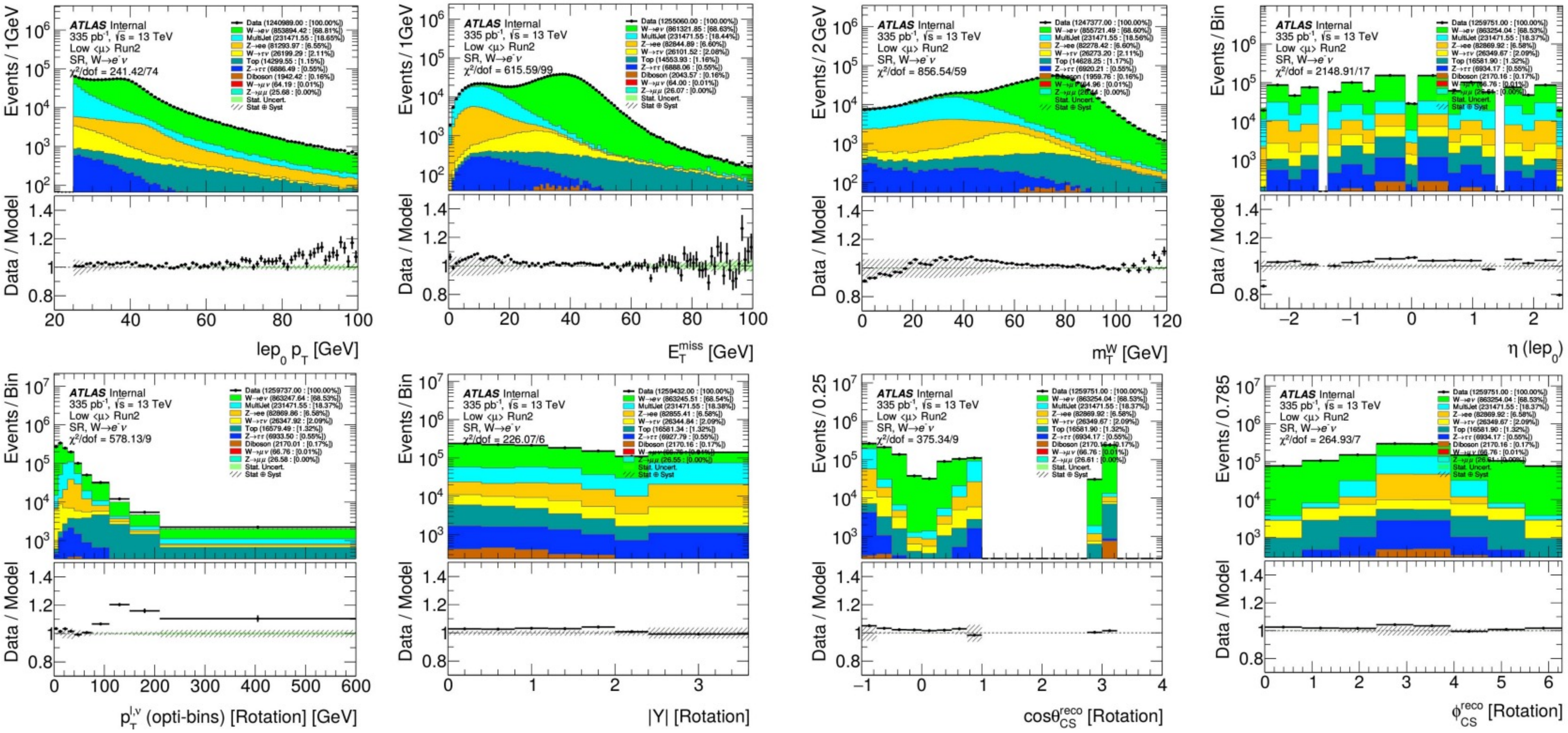

Control plots in the Signal Region for $W^{-} \rightarrow \mu^{-}\nu$

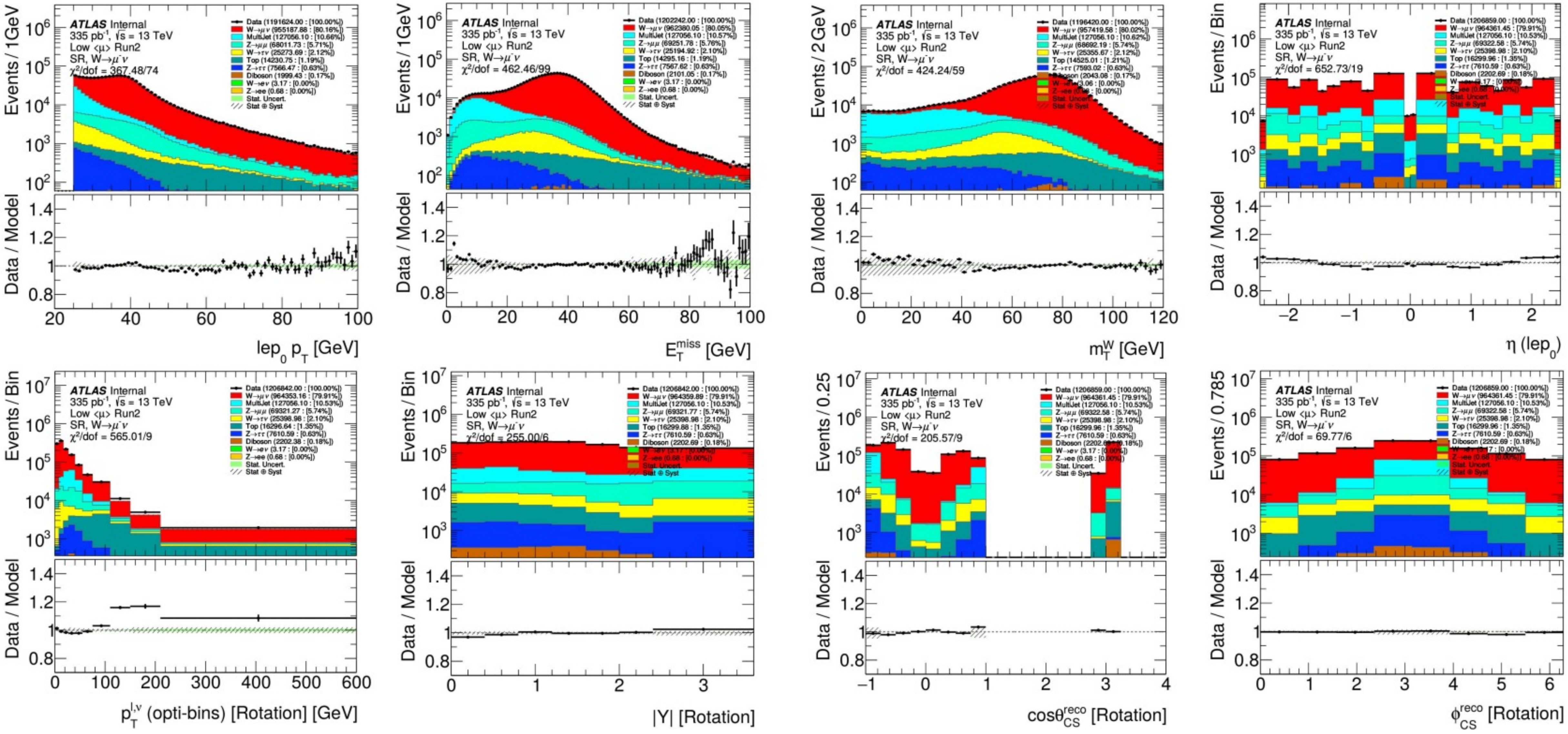

Fitting method

Reference coefficients created by taking moments of the polynomials using truth MC

$$\langle P_i(\theta,\varphi)\rangle = \frac{\int d\sigma(p_T,m,y,\theta,\varphi)\,P_i(\theta,\varphi)\,d\cos\theta d\varphi}{\int d\sigma(p_T,m,y,\theta,\varphi)\,d\cos\theta d\varphi}$$

$$\langle\cos\theta\rangle = \frac{1}{4}A_4$$

Truth phase space is folded into the reco phase space through polynomial templates.

$$T_{ij} = \sum_{event\in\Delta_j} \frac{P_i\left(\cos\theta_{CS}^{Reco},\varphi_{CS}^{Reco}\right) w_{event}(r,t)}{\sigma_j\left\{P_8\left(\cos\theta_{CS}^{Truth},\varphi_{CS}^{Truth}\right)+\sum_{i=0}^{7}A_{ij}^{ref}P_i\left(\cos\theta_{CS}^{Truth},\varphi_{CS}^{Truth}\right)\right\}}$$

Extraction of coefficients through likelihood fit of MC templates in $p_T^{l,\nu}$ and $y^{l,\nu}$ bins.

$$\mathcal{L}(A_{ij},\mu_j|N) = \prod_{events}^{N}\left\{\sum_{j=1}^{N_{p_T}^{bins}}\mu_j\left[T_{8,j}+\sum_{i=0}^{7}A_{ij}\times T_{ij}\right]+\sum_{B}^{bkgds}T_B+T_{Fakes}\right\}$$

Polynomial templates differ to ZAi analysis by extending $\cos\theta_{CS}$ range to save information for events with no real solution.

Systematics

- Have largest expected systematics included (MJ, cross-section variation, hadronic recoil, and MC stat) and understood.
- Adding remaining systematics (PDF[1] and lepton)
- Large constraint on MJ systematics from very conservative estimation[2].

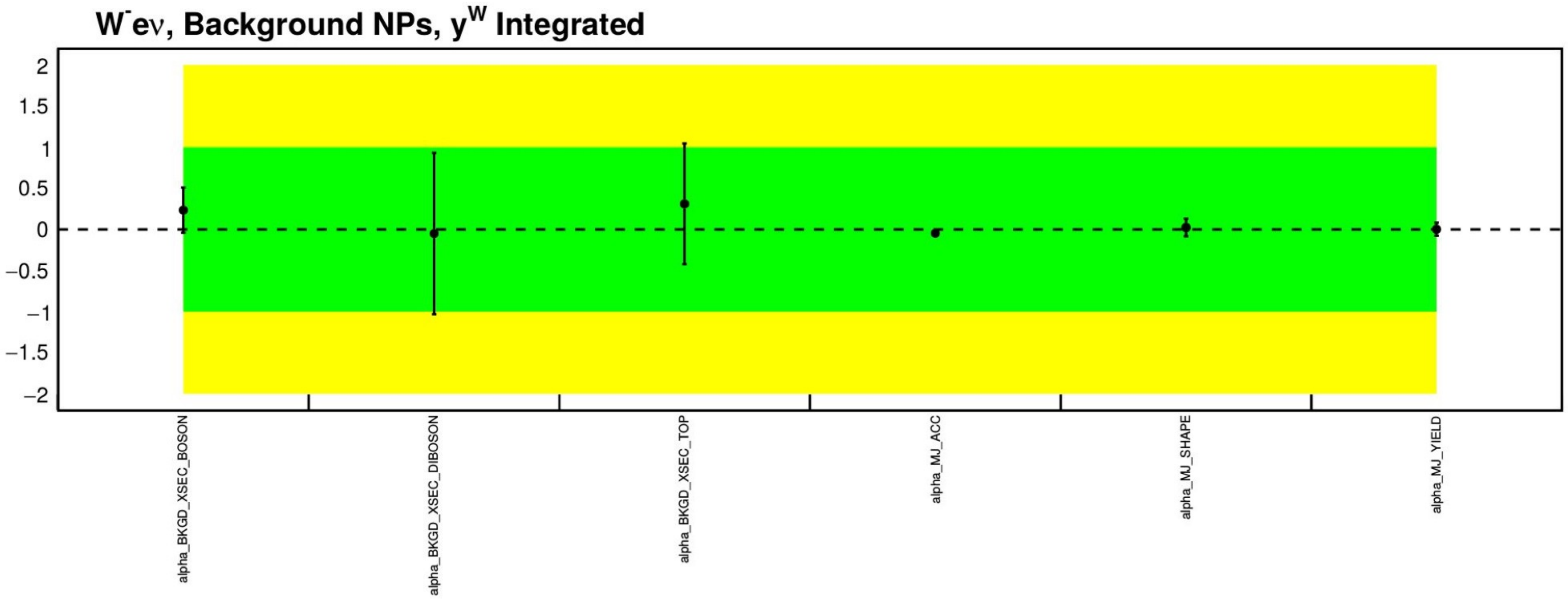

Systematics

$W^{-}e\nu$ NPs, $pt^{e\nu}$ Binning

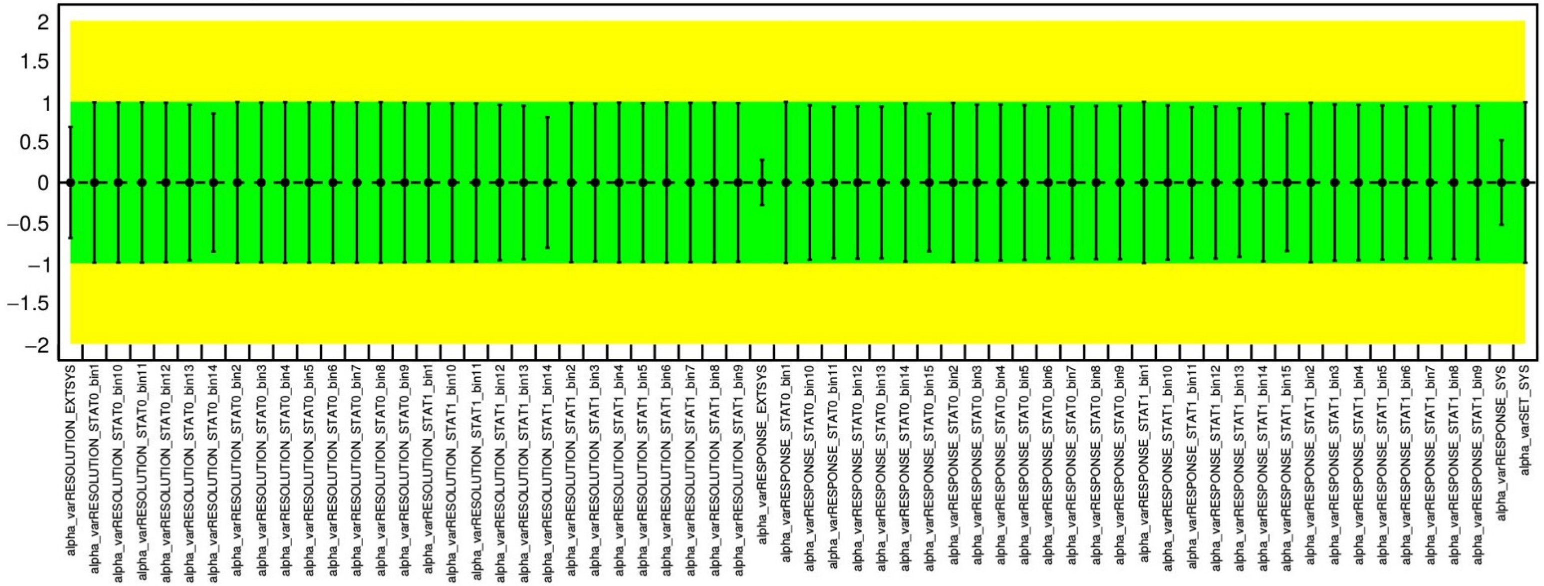

$W^{-}CC$ NPs, pt^{CC} Binning

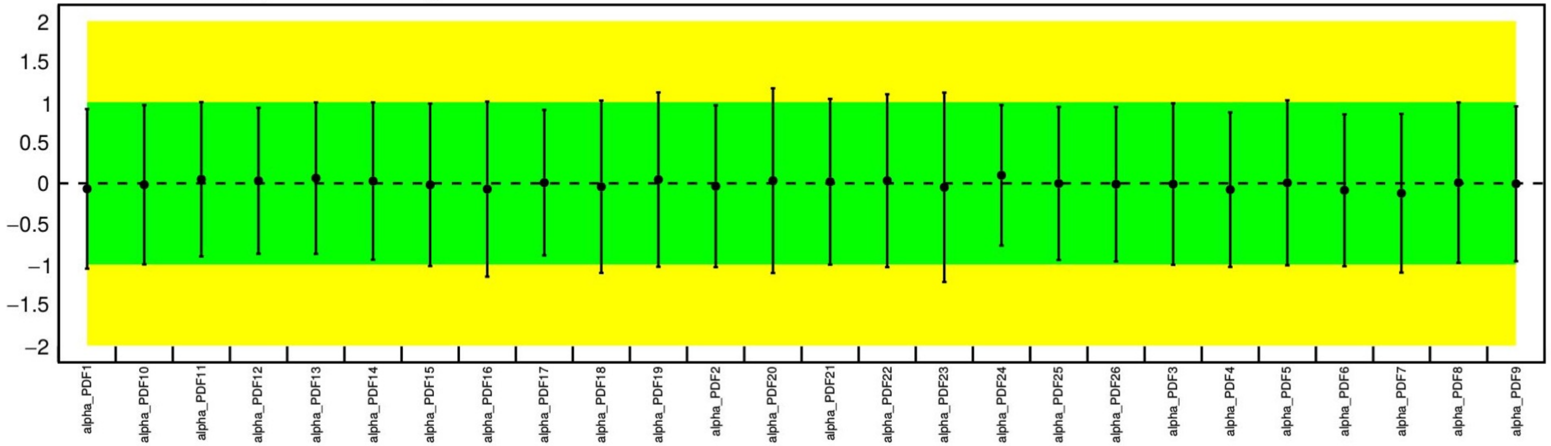

Pseudo data ($p_T^{l,\nu}$)

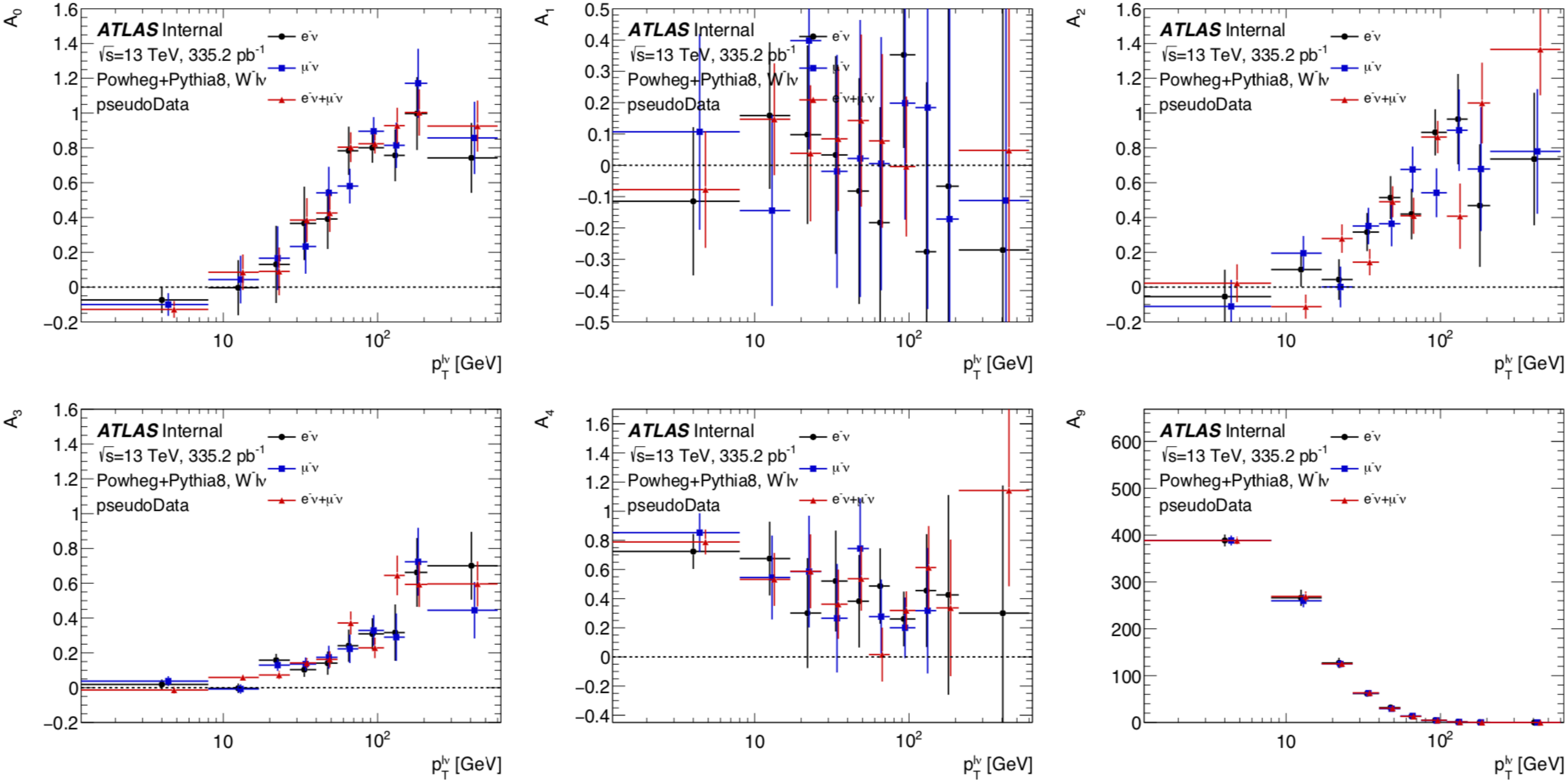

Systematic uncertainties ($p_T^{l,\nu}$)

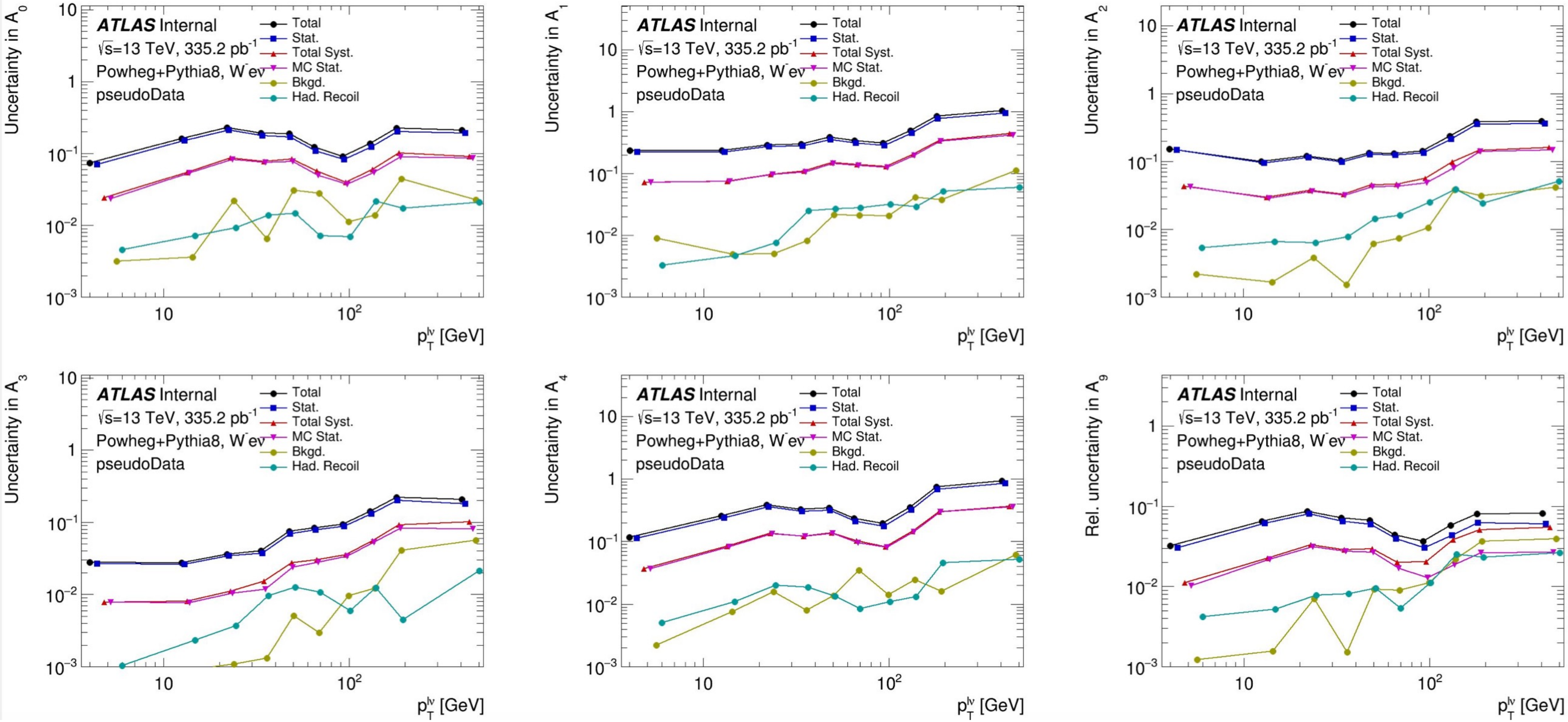

- Expect uncertainty to be stat dominated for all bins for both p^W and y^W differential measurements

Pseudo data ($y^{l,\nu}$)

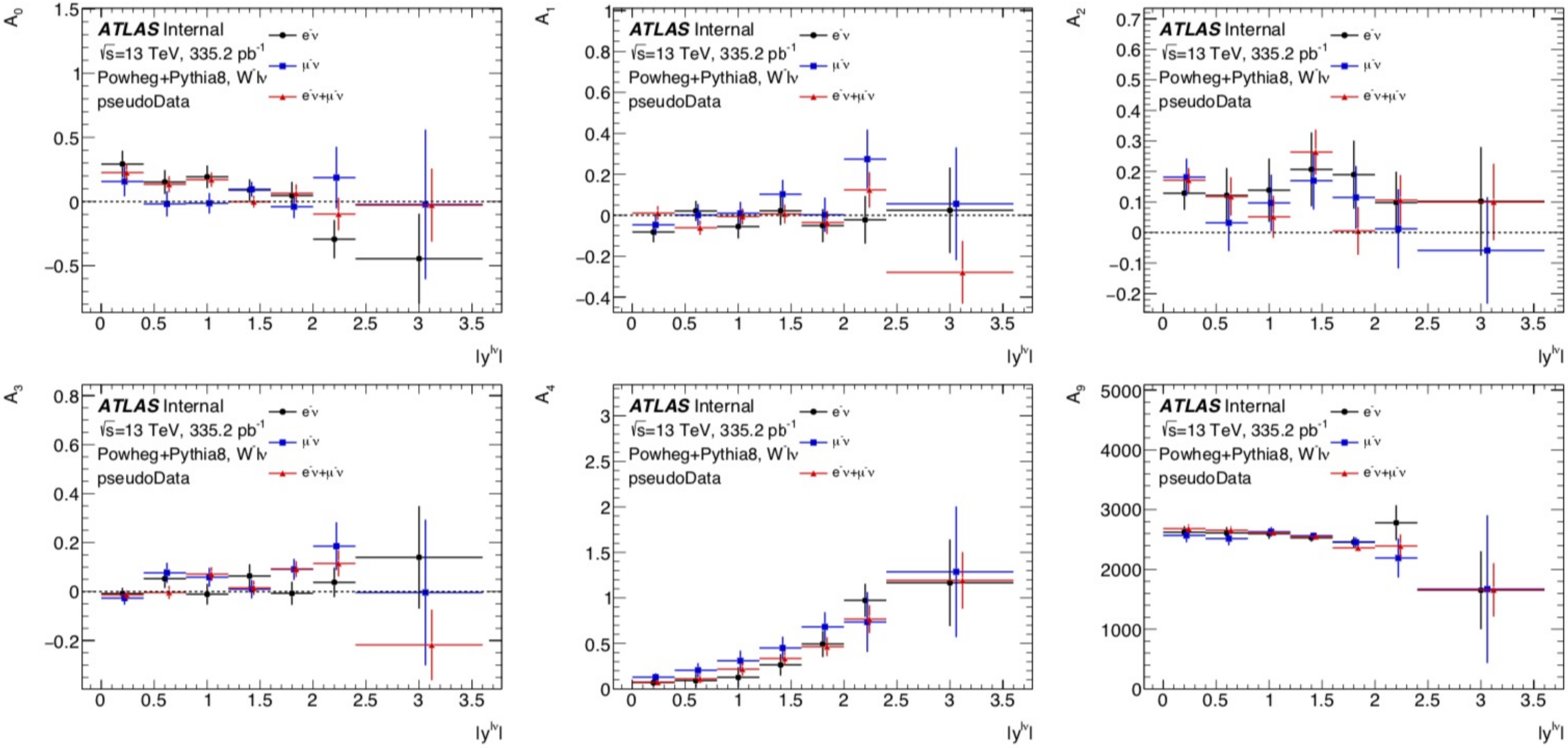

Systematic uncertainties ($y^{l,\nu}$)

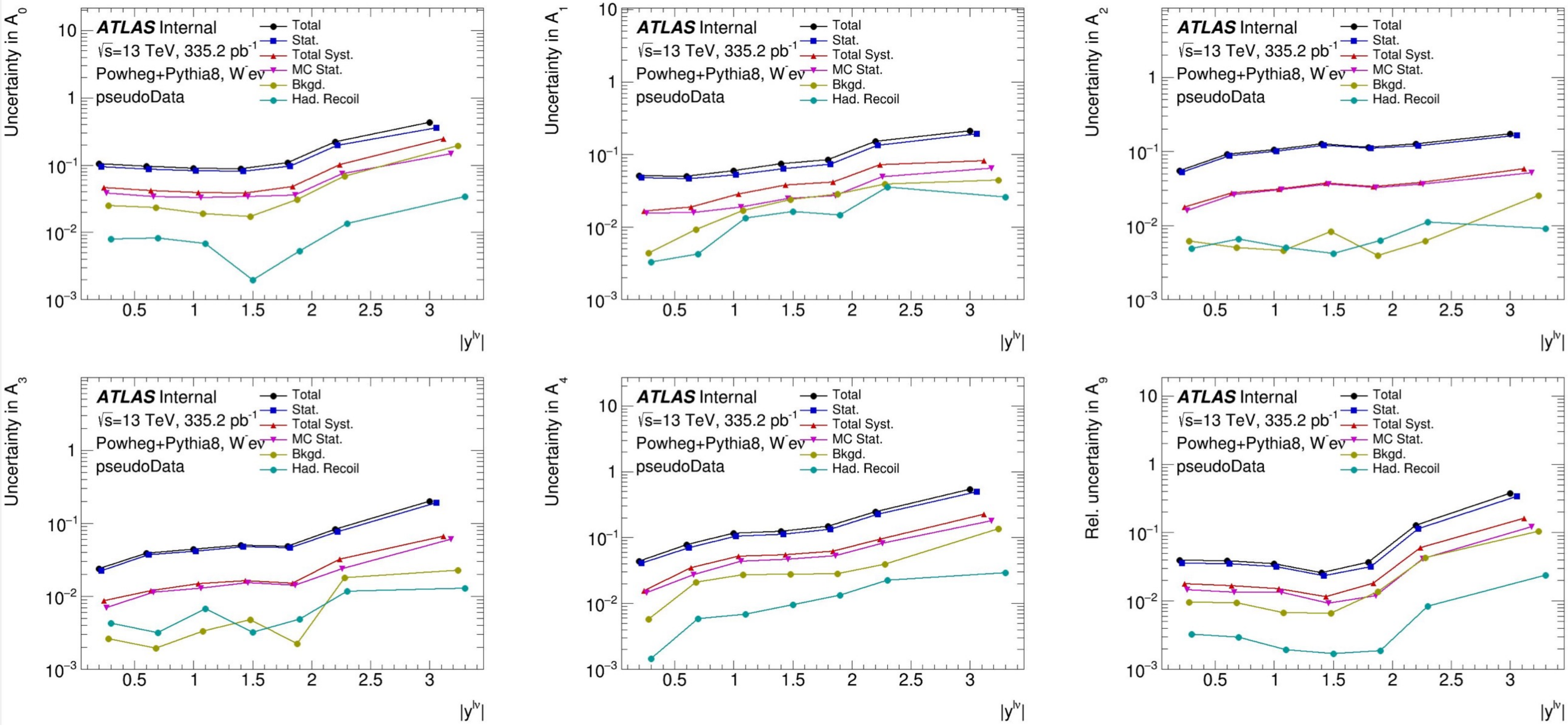

- Expect uncertainty to be stat dominated for all bins for both p^W and y^W differential measurements

Current status

- Goal of the measurement
  - measure A_i in W events
  - important input to W mass measurement and PDF fits
  - main targets: A_4 (forward-backward asymm.), $A_0 - A_2$ (Lam-Tung), charge asymmetry
- Measurement status:
  - Use W events in low-μ data (less statistics, but better hadronic recoil resolution)
  - Solve for neutrino p_z via W mass constraint
  - Study of sensitivity of this analysis to A_4
  - MJ background estimate is in place. Other backgrounds added and understood.
  - Inclusion of hadronic recoil systematics and background systematics.
  - Electron and muon channel combined fit also working.
- ToDo:
  - Refine MJ systematics correlation uncertainty model (MJ NPs heavily constrained, still being understood)
  - Fit doesn’t work with real data
  - Add remaining systematics
  - Prepare for EB request

MJ estimation updates

MJ background in WAi analysis (1): inclusive SR

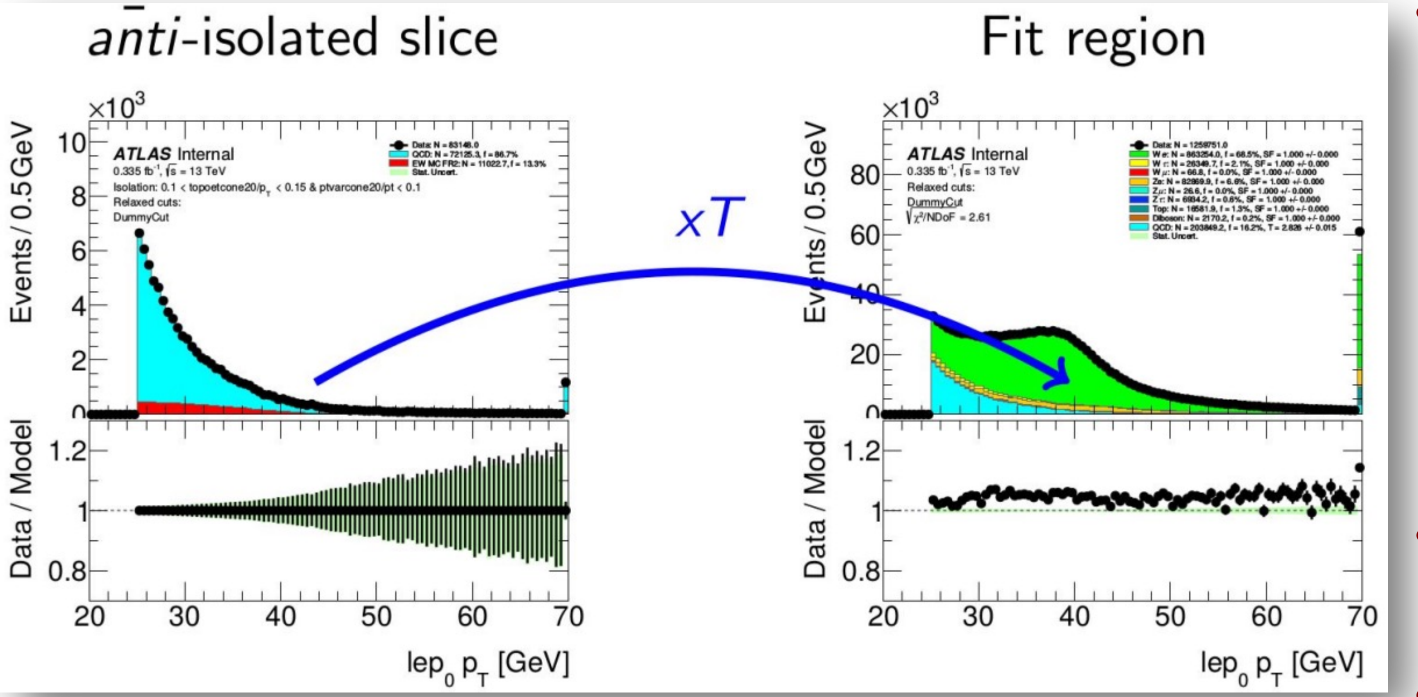

- Calorimetric isolation used for e± and track isolation used for μ± channels:
  - Slicing ptvarcone20/pt for W→μν: 8 slicing bins from 0.1 to 0.5
  - Slicing in topoetcone20/pt for W→eν: 8 slicing bins from 0.05 to 0.45

- MJ bkgd estimate has 2 "steps":
  - Calculate MJ normalization
    - Repeat MJ estimation for different anti-isolation slices
    - Fit linear function
    - Extrapolate back to SR
  - Calculate MJ template shape:
    - MJ distributions in anti-iso slices don't match SR shape
    - Apply bin-by-bin linear shape extrapolation
    - Assign 100% uncertainty
- Use 4 discriminative variables:
  - $p_T^l, m_T, E_T^{miss}, |\Delta\varphi(l, E_T^{miss})|$
- In the fit use fixed EWT background normalization.
- To get MJ shape as a function of |Y| and $p_T^{l,\nu}$ following samples used:
  - $b\bar{b} + c\bar{c}$ for W→μν channels
  - JF17 for W→eν channels

MJ background in WAi analysis (2): inclusive SR

MJ normalization

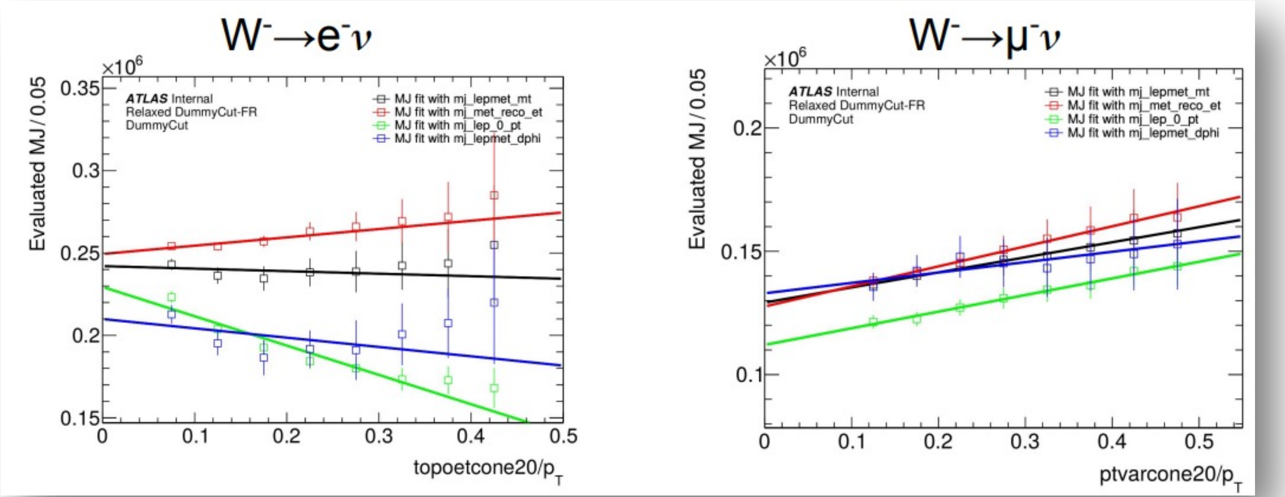

- The error bars are multiplied by $\sqrt{\chi^2/NDoF}$
- Take final MJ yield as mean at $ptvarcone20/pt$=0.025
- Less MJ background contribution for muon channel (as expected).
- Dominant MJ yield uncertainty comes from intersection point.

MJ template shape

In assumption, extrapolation is linear:

$$H_{MJ}^{[0.A,0.B]}[X] = H_{Data}^{[0.A,0.B]}[X] - H_{MC}^{[0.A,0.B]}[X]$$

$$\Delta H[X] = \frac{1}{4}\left\{\frac{H_{MJ}^{0.1,0.15} - H_{MJ}^{0.3,0.35}}{4} + \frac{H_{MJ}^{0.15,0.2} - H_{MJ}^{0.35,0.4}}{4} + \frac{H_{MJ}^{0.2,0.25} - H_{MJ}^{0.4,0.45}}{4} + \frac{H_{MJ}^{0.25,0.3} - H_{MJ}^{0.45,0.5}}{4}\right\}$$

$$H_{MJ}^{sig}[X] = H_{MJ}^{0.1,0.15}[X] + 2 \cdot \Delta H[X]$$

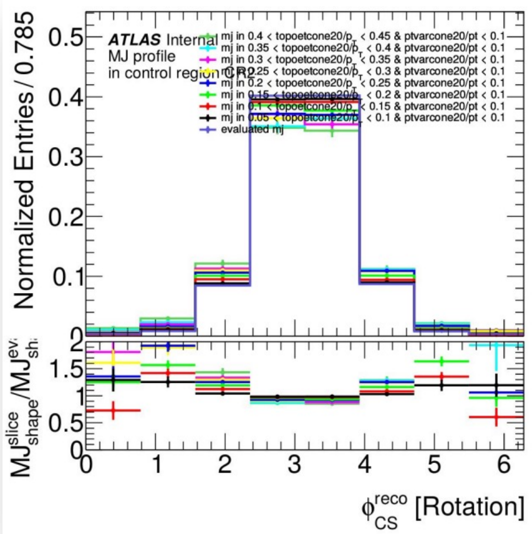

- Calculate shape correction using isolation slices for final MJ templates.
- Given the large statistical uncertainty and the linear approximation used, the shift ΔH[X] applied is assigned a 100% relative uncertainty.
  - Small wrt intersection point.

MJ Systematics Summary (inclusive signal region)

Channel	Using *topoetcone20*/p_T $W \to e^- \nu$	Using *topoetcone20*/p_T $W \to e^+ \nu$	Using *ptvarcone20*/p_T $W \to \mu^- \nu$	Using *ptvarcone20*/p_T $W \to \mu^+ \nu$
Total Number of MJ bkg	**231472**	**232268**	**127056**	**132995**
Luminosity and cross section	±7199 (3.11%)	±9098 (3.92%)	±547 (0.43%)	±698 (0.52%)
Intersection point	±22928 (9.91%)	±24910 (10.72%)	±13313 (10.48%)	±12276 (9.23%)
Extrapolation target	±1246 (0.54%)	±1172 (0.50%)	±1575 (1.24%)	±1433 (1.08%)
Choice of hists	±7643 (3.30%)	±8303 (3.57%)	±4438 (3.49%)	±4092 (3.08%)
Isolation correction	N/A	N/A	N/A	N/A
Correlated Uncertainty	±24032 (10.38%)	±26519 (11.42%)	±13324 (10.49%)	±12296 (9.25%)
Data Stat.	±490 (0.21%)	±463 (0.20%)	±795 (0.63%)	±809 (0.61%)
MC Stat.	±262 (0.11%)	±229 (0.10%)	±990 (0.78%)	±880 (0.66%)
Shape Correction	±2961 (1.28%)	±2769 (1.19%)	±927 (0.73%)	±915 (0.69%)
Uncorrelated Uncertainty	±3012 (1.30%)	±2816 (1.21%)	±1572 (1.24%)	±1505 (1.13%)

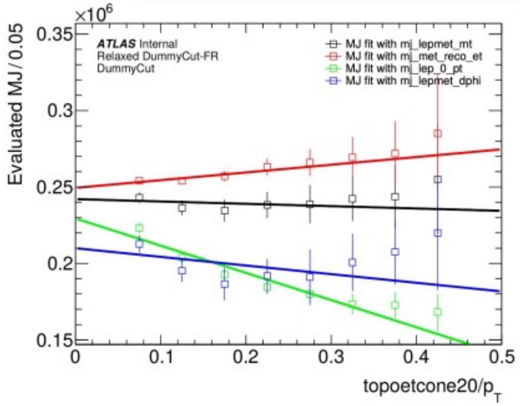

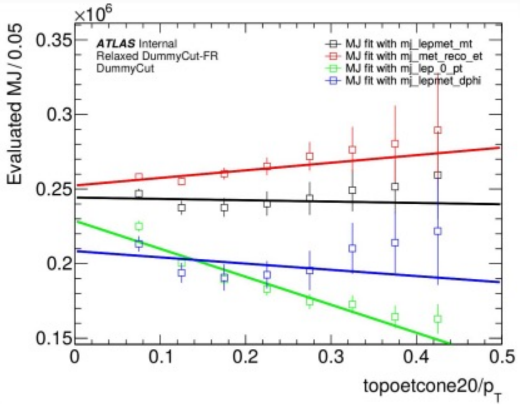

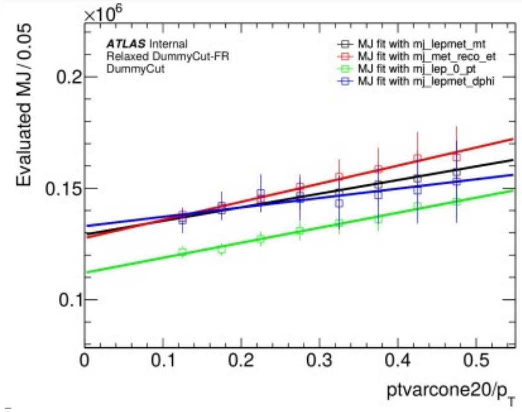

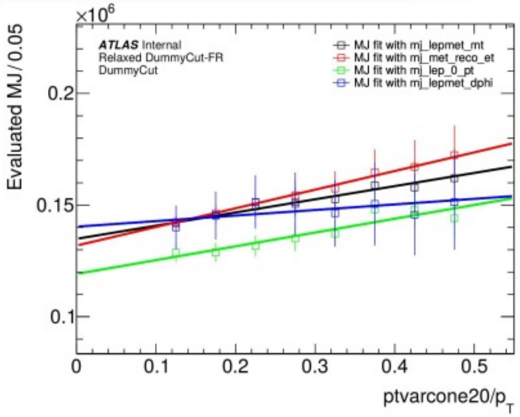

MJ templates for $\cos\theta_{CS}$ vs. φ_{CS} : inclusive SR

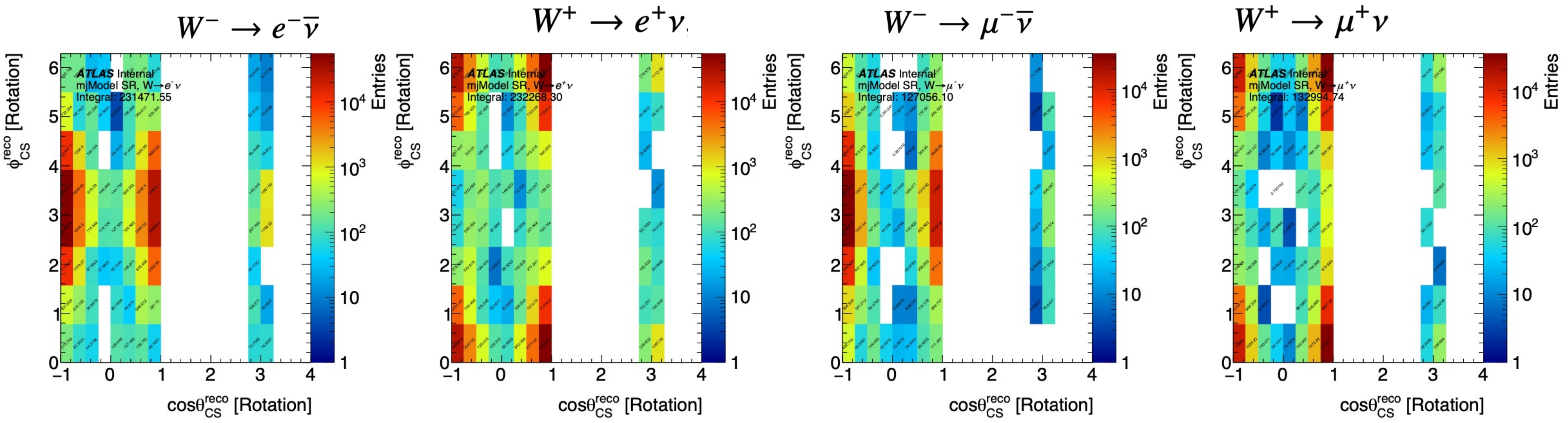

- The 2D templates are derived in the same way as described for 1D histograms

MJ shape as function of |Y| and $p_T^{l,\nu}$: task definition

1D control plots in SR (only stat unc. + MJ systematics are shown.):

$W^- \to e^- \nu$ $\qquad\qquad$ $W^- \to \mu^- \nu$

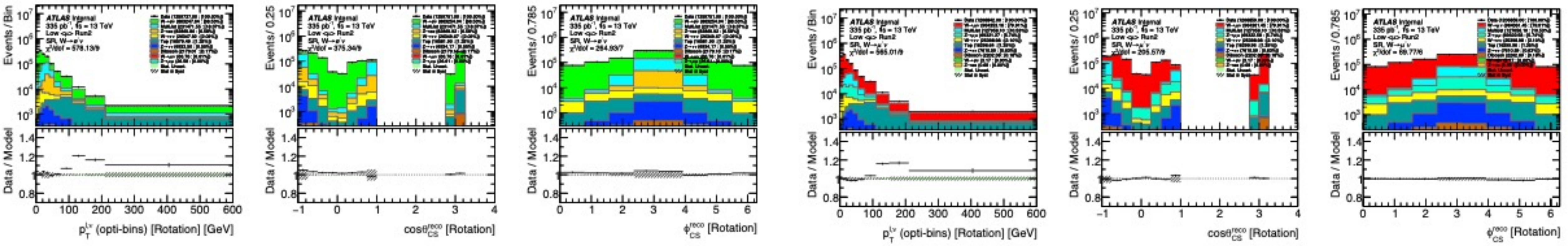

W-Ai analysis uses more complicated approach:

- Building 2D histograms $\cos\theta_{CS}$ vs. ϕ_{CS} as function of η or $p_T^{\ell,\nu}$

$$p_T^{\ell,\nu} : [0, 8, 17, 27, 40, 55, 75, 110, 150, 210, 600];$$
$$|Y| : [0, 0.4, 0.8, 1.2, 1.6, 2.0, 2.4, 3.6]$$

- Above 100 GeV the data/MC agreement in the $p_T^{\ell,\nu}$ degradate due to missing truth p_T^W reweighting correction above this range.

Closure test by DD method: coarse bins

$p_T^{\ell,\nu}$: [0, 17, 55, 600];
$|Y|$: [0, 0.8, 2.0, 3.6]

$W^- \to e^- \overline{\nu}$

$W^- \to \mu^- \overline{\nu}$

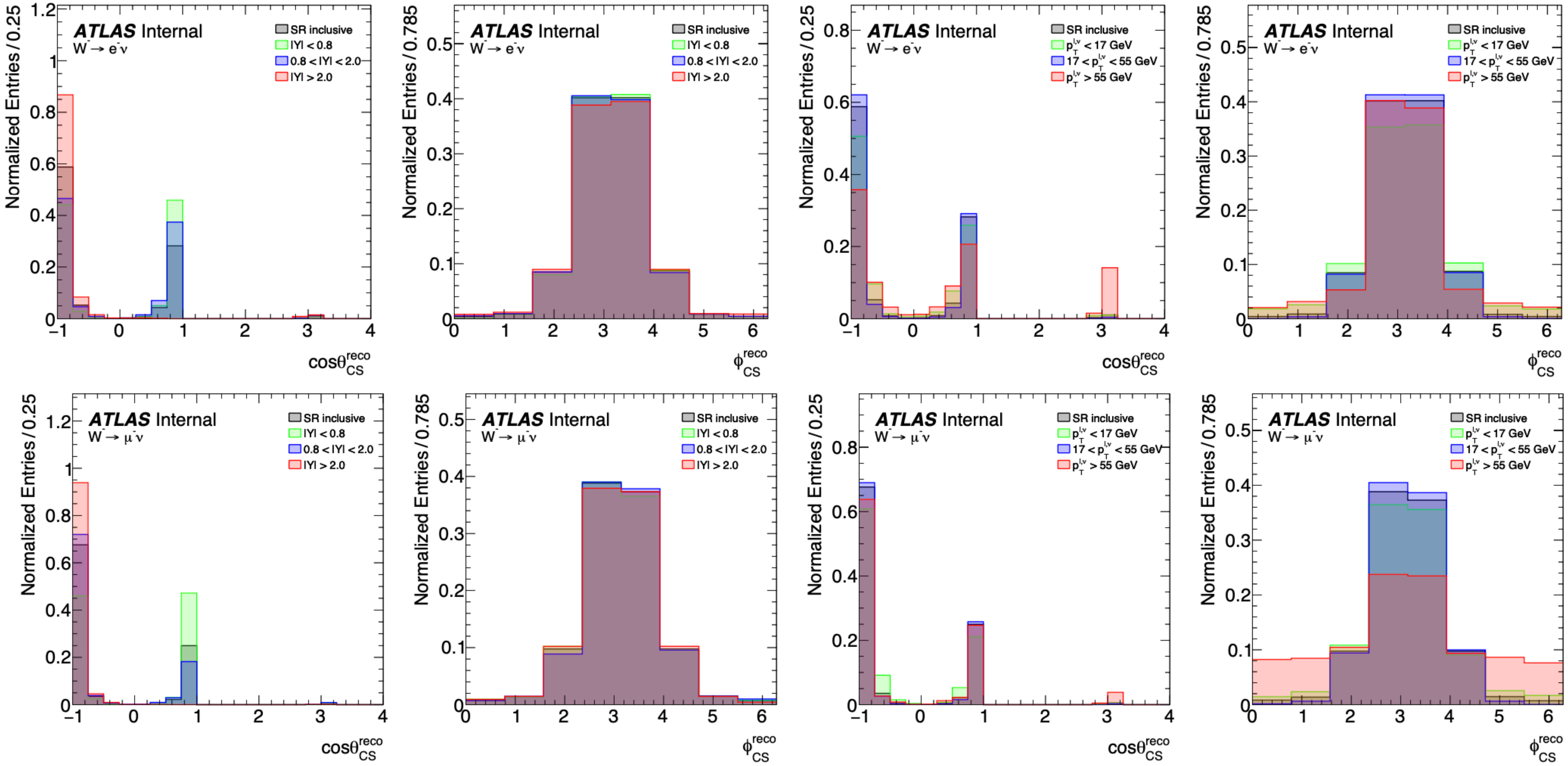

MJ shape as function of |Y| and $p_T^{l,\nu}$: studies

$p_T^{\ell,\nu}$: [0, 17, 55, 600];
$|Y|$: [0, 0.8, 2.0, 3.6]

- There are strong dependence of the $\cos\theta_{CS}$ MJ template shape as function of $|Y^{l,v}|$ and φ_{CS} as a function of $p_T^{l,\nu}$
- Acceptance correction functions were built to correct MJ data-driven template derived in the SR to the given $|Y^{l,v}|$ or $p_T^{l,\nu}$ slice using the samples:
  - $b\bar{b} + c\bar{c}$ for W→μν channels
  - JF17 for W→eν channels

$$A_j = h_{MC}^{bin_j} / h_{MC}^{SR} \qquad h_{MJ}^{bin_j} = h_{MJ,data}^{SR} \times A_j$$

- Acceptance correction functions for number of $|Y^{l,v}|$ bins, fully uncorrelated uncertainty on these acceptance correction functions is applied on the MJ estimate:

Data-driven MJ derived for 3 individual regions in |Y|:

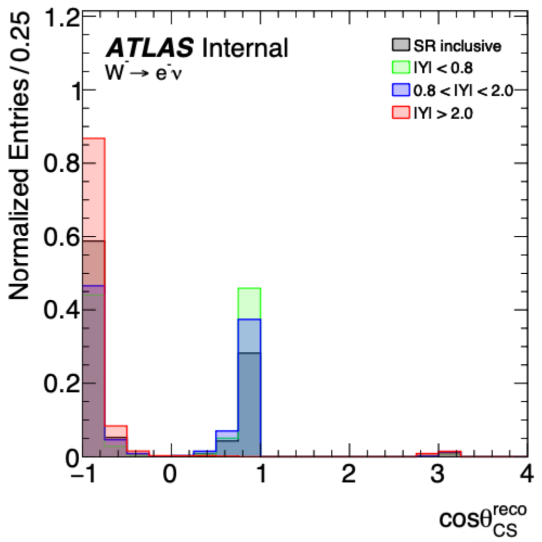

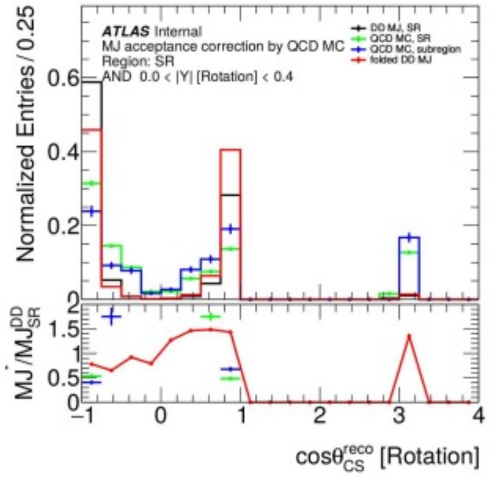

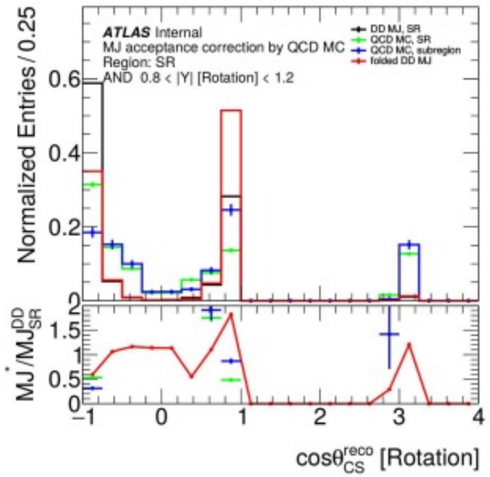

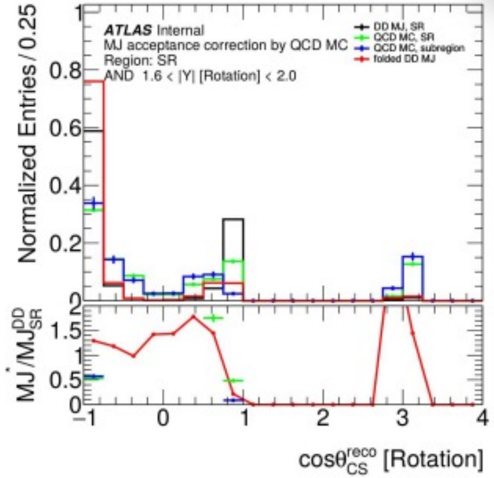

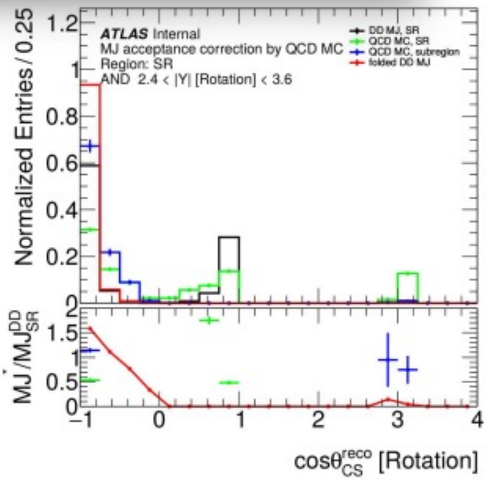

Acc. corr. function: closure test

$p_T^{\ell,\nu}$: [0, 17, 55, 600];
$|Y|$: [0, 0.8, 2.0, 3.6]

$W^- \to e^- \overline{\nu}$

$W^- \to \mu^- \overline{\nu}$

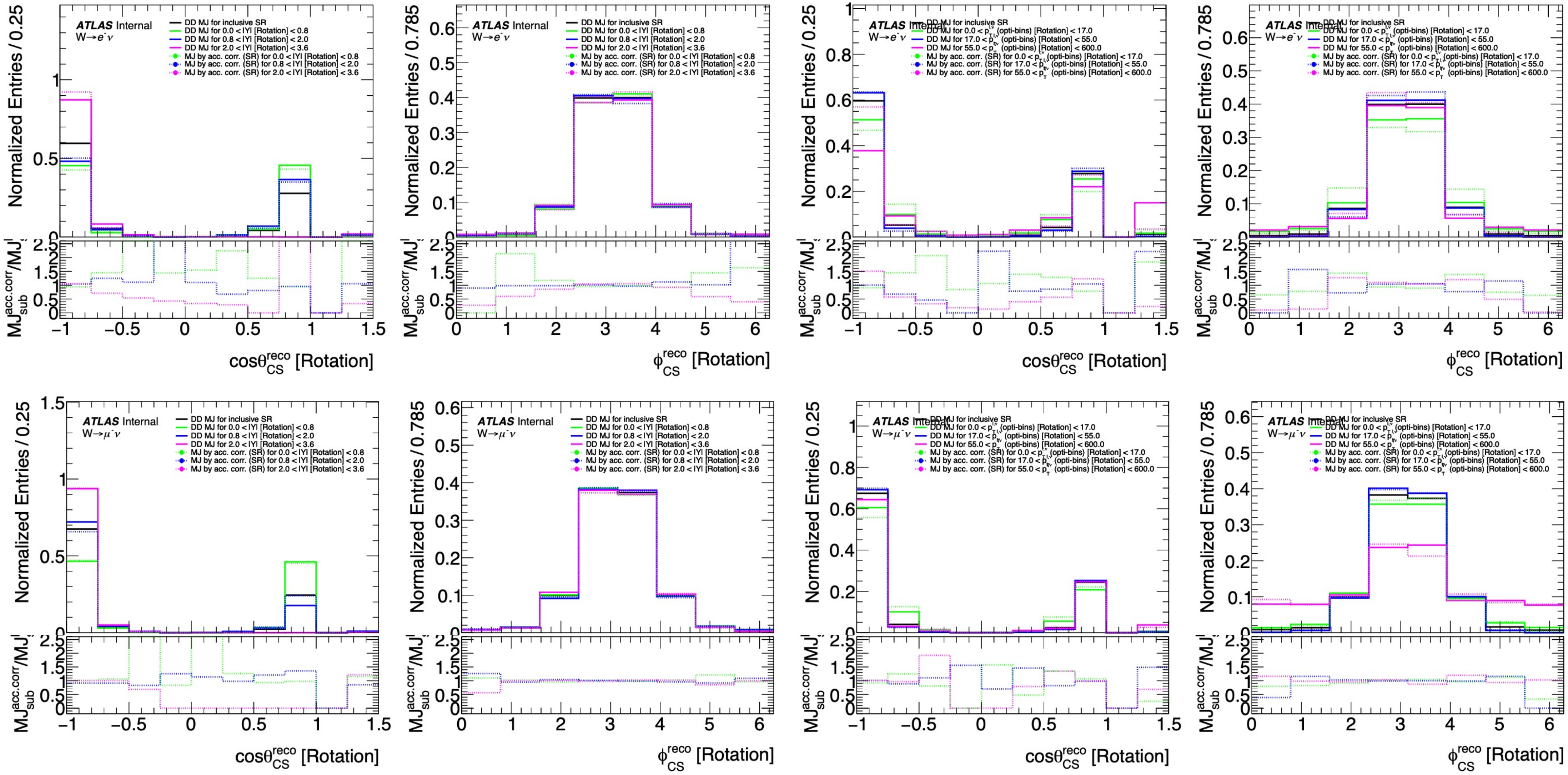

MJ shape as function of $|Y|$ and $p_T^{\ell,\nu}$

- There are strong dependence of the $\cos\theta_{CS}$ MJ template shape as function $|Y|$ and ϕ_{CS} as function of $p_T^{\ell,\nu}$
- Acceptance correction functions were build using QCD MC samples to correct MJ data-driven template derived in the SR to the given $|Y|$ or $p_T^{\ell,\nu}$ slice:
  $h_{MJ}^{bin_i} = h_{MJ}^{SR} \cdot h_{QCDMC}^{bin_i} / h_{QCDMC}^{SR}$

Closure test for Data-driven MJ and Acc.Corr MJ derived for 3 individual regions in $p_T^{\ell,\nu}$:

$W^- \to e^- \nu$ $\qquad$ $W^- \to \mu^- \nu$

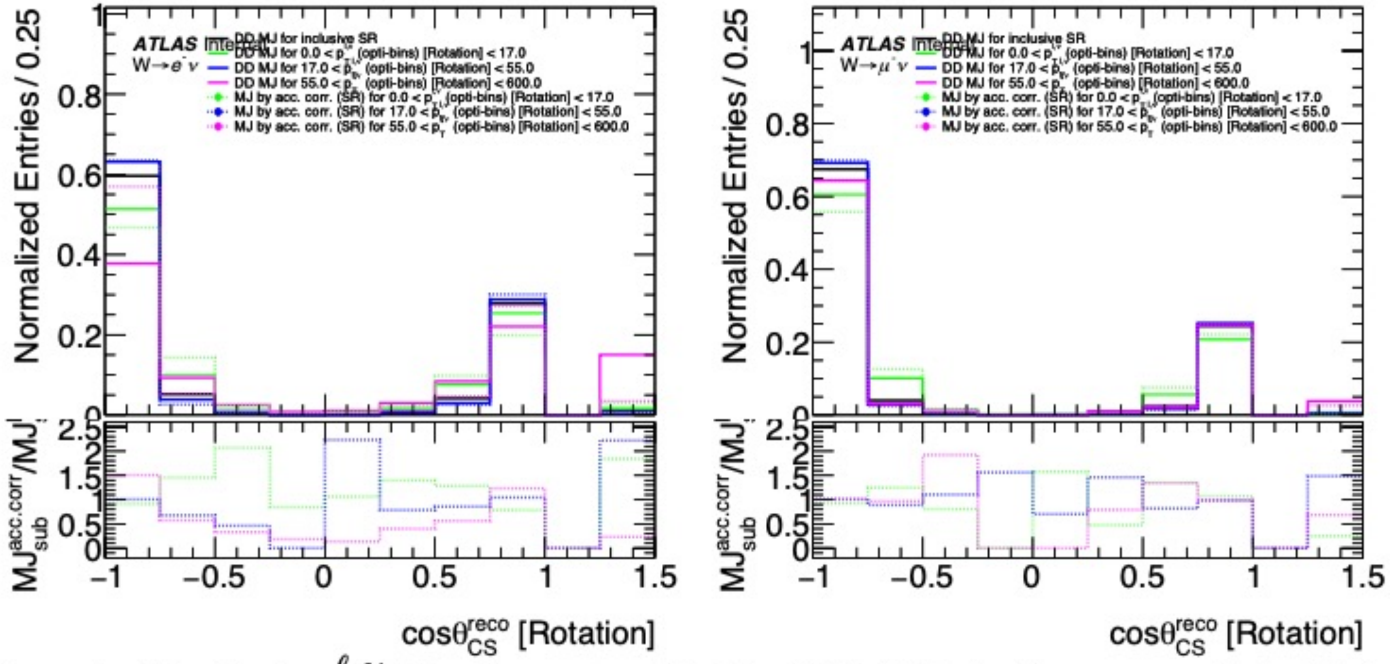

Problem:

- Comparing to MJ template given by AccCocc in the last $p_T^{\ell,\nu}$ bin for e^- with the DD MJ, last one predicts higher MJ contribution to the no solution bin + overall shape differs a lot.
- **DD MJ template derived from SR might be "too far" from DD MJ template derived for $p_T^{\ell,\nu} > 55$ GeV bin.**
- We might not see this effect in muons due to the fact this channel is "cleaner".
- Integrated distributions for Y coarse bins looks good due to small MJ fraction for the last coarse $p_T^{\ell,\nu}$ bin.

Solution:

- Instead of using SR use the coarse bins: $h_{QCDMC}^{CoarseBin_k}$ and $h_{MJ}^{CoarseBin_k}$.

$p_T^{\ell,\nu}$: $[0, 17, 55, 600]$;
$|Y|$: $[0, 0.8, 2.0, 3.6]$

Some W-Ai control plots and e/μ compatibility

Compare 2 $p_T^{\ell,\nu}$ bins: $17 < p_T^{\ell,\nu} < 27$ GeV and $150 < p_T^{\ell,\nu} < 210$ GeV

Before

$17 < p_T^{\ell,\nu} < 27$ GeV

$150 < p_T^{\ell,\nu} < 210$ GeV

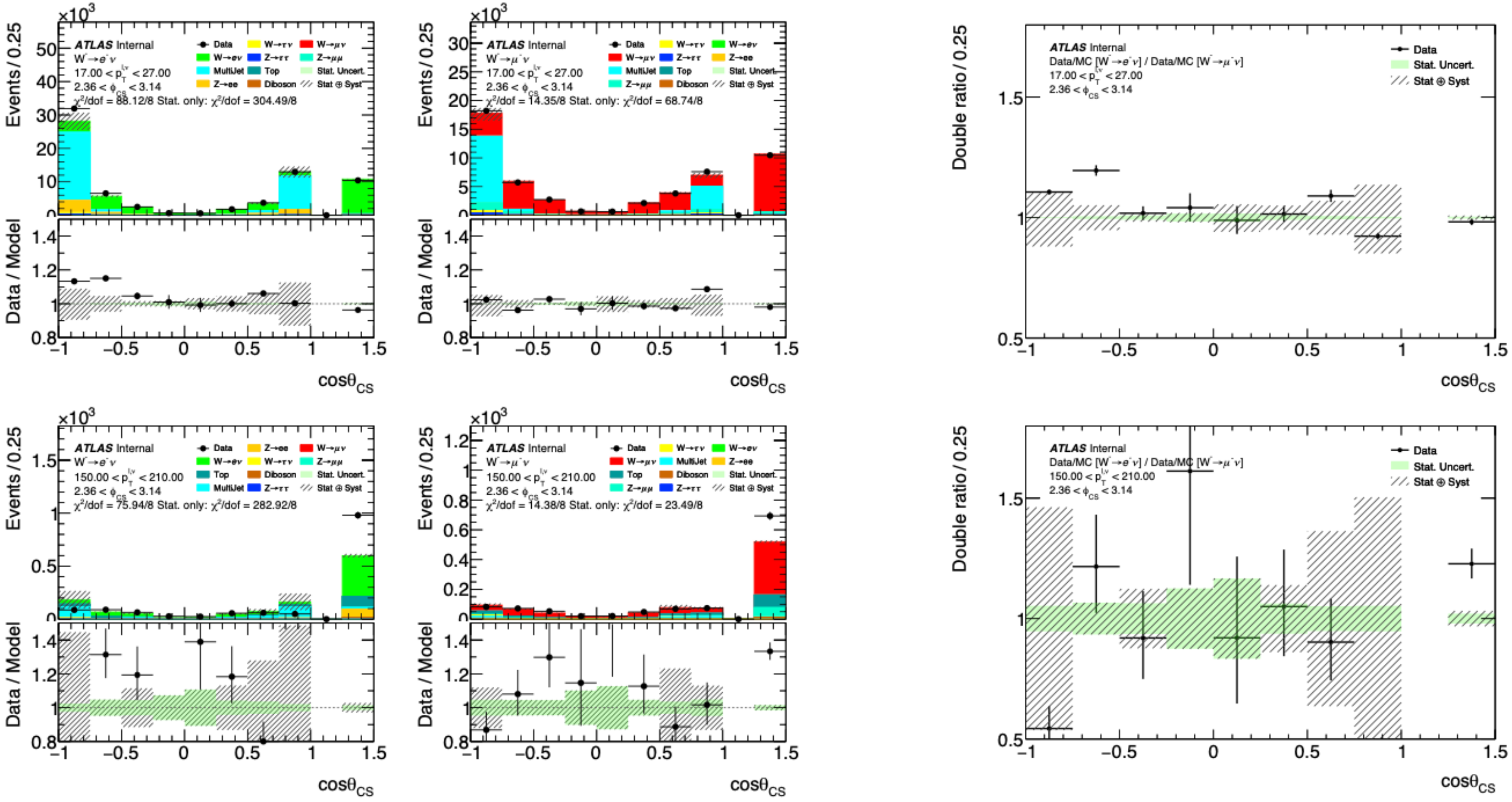

Note: discrepancy in the no solution bins in pTW>100 GeV is from absence of the PTRW

Test with 1D $\cos\theta_{CS}$ integrated over ϕ_{CS} in some $p_T^{\ell,\nu}$ bins

Instead of using SR, use the coarse bins: $h_{QCDMC}^{CoarseBin_k}$ and $h_{MJ}^{CoarseBin_k}$.

Before

After

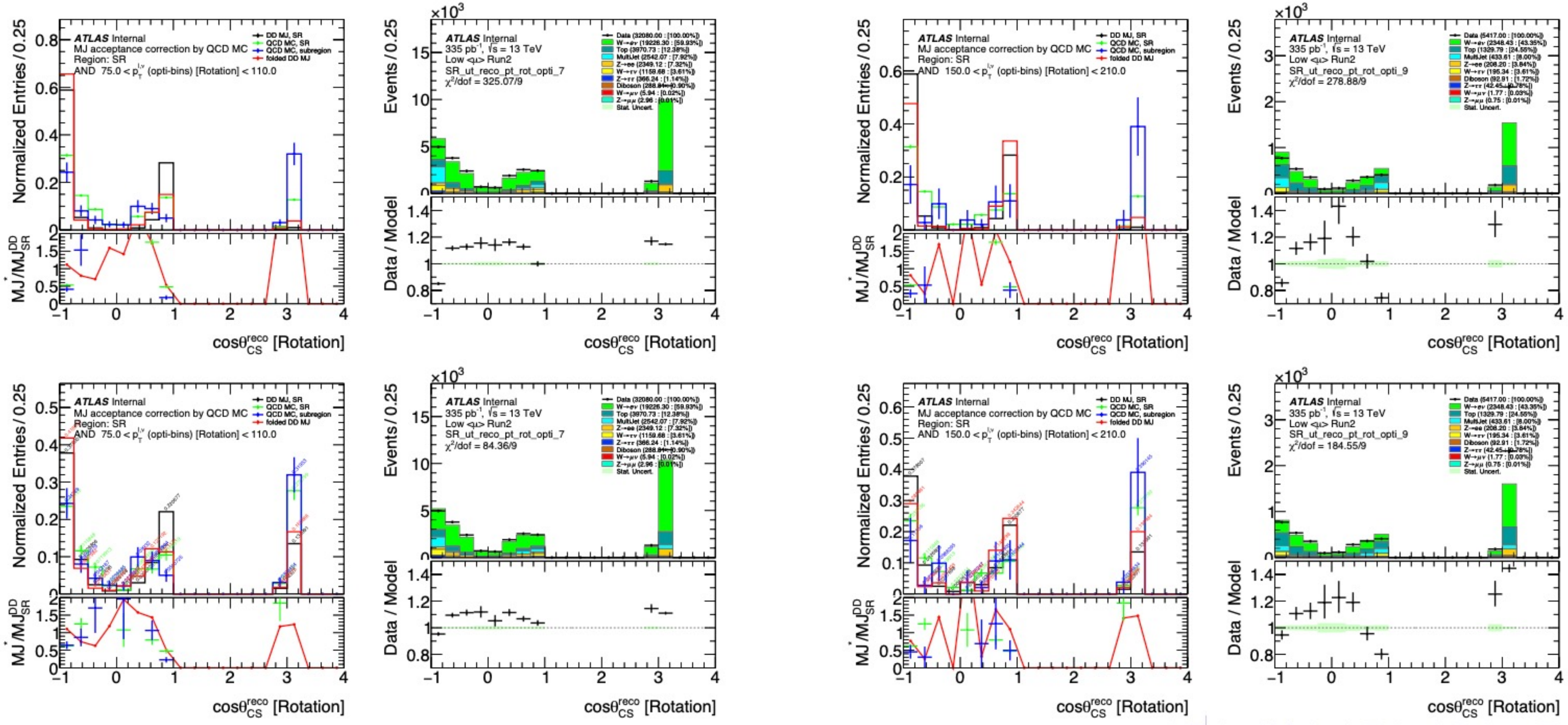

Note: discrepancy in the no solution bins in pTW>100 GeV is from absence of the PTRW

Test with 3D W-Ai control plots

Before

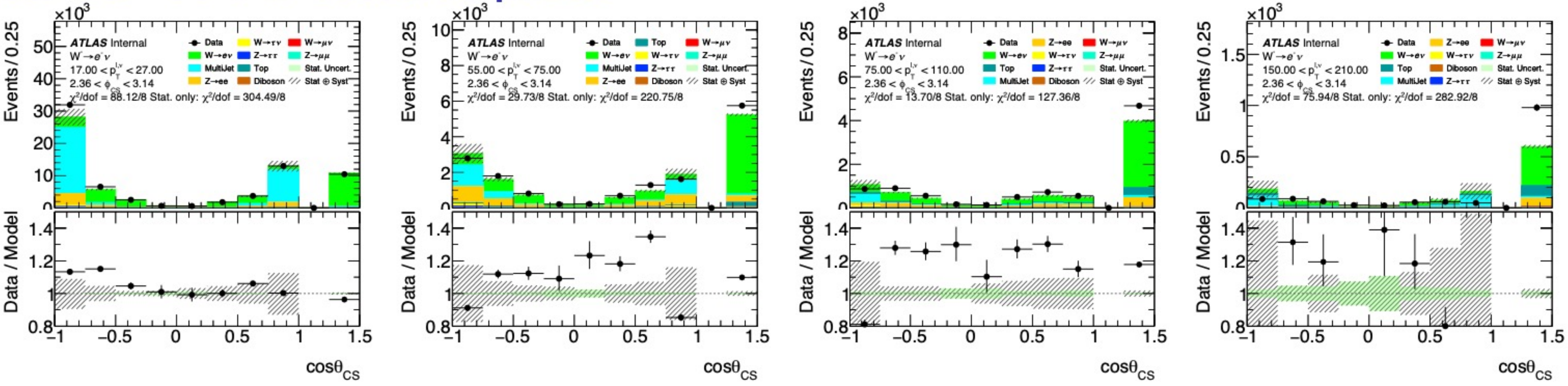

After

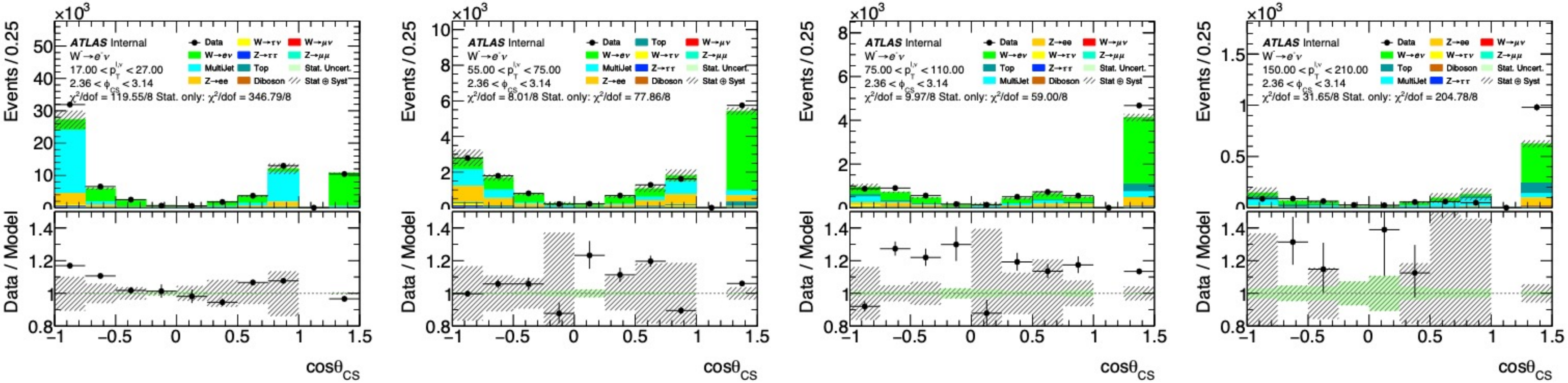

Only some $p_T^{\ell,\nu}$ coarse bins and ϕ_{CS} slices are shown.

Note: discrepancy in the no solution bins in pTW>100 GeV is from absence of the PTRW

MJ templates for W-Ai analysis in $p_T^{l,\nu}$ binnning $W^- \to e^- \overline{\nu}$

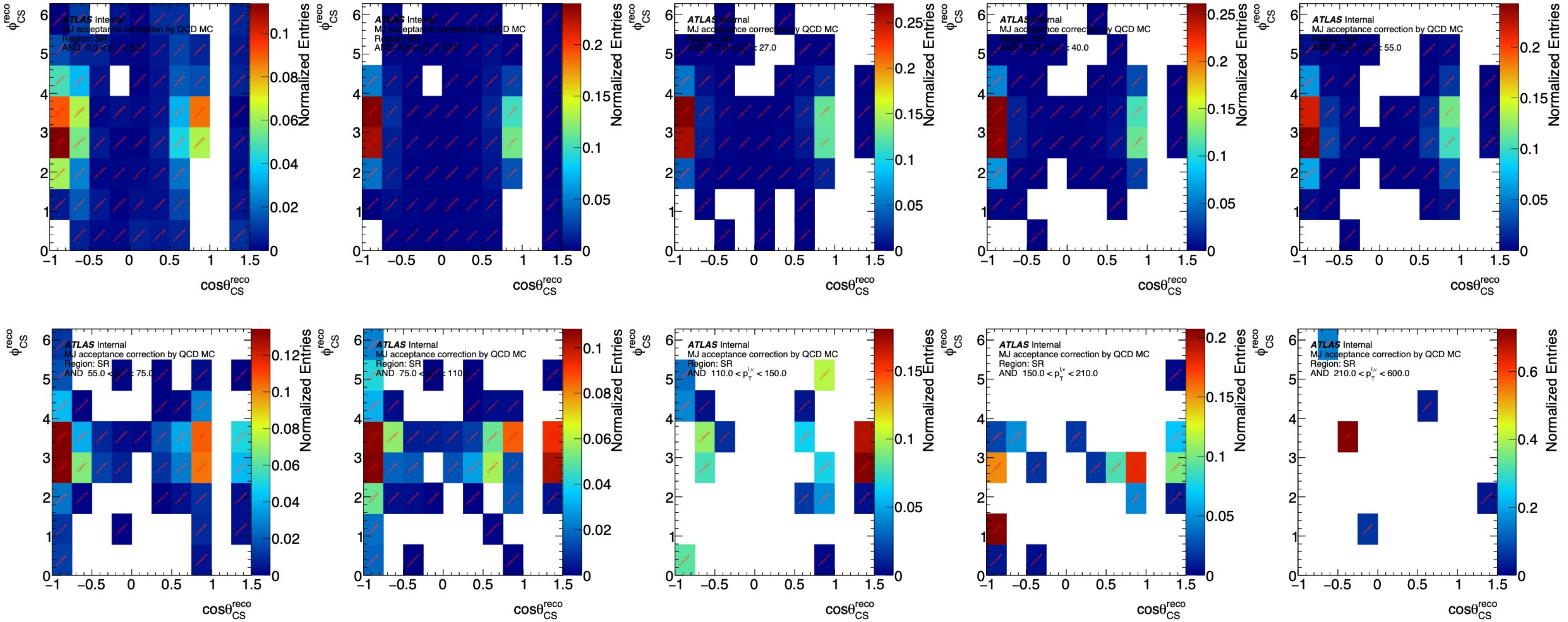

$$p_T^{\ell,\nu} : [0, 8, 17, 27, 40, 55, 75, 110, 150, 210, 600];$$

MJ templates for W-Ai analysis in $|Y|$ binnning $W^- \to e^- \bar{\nu}$

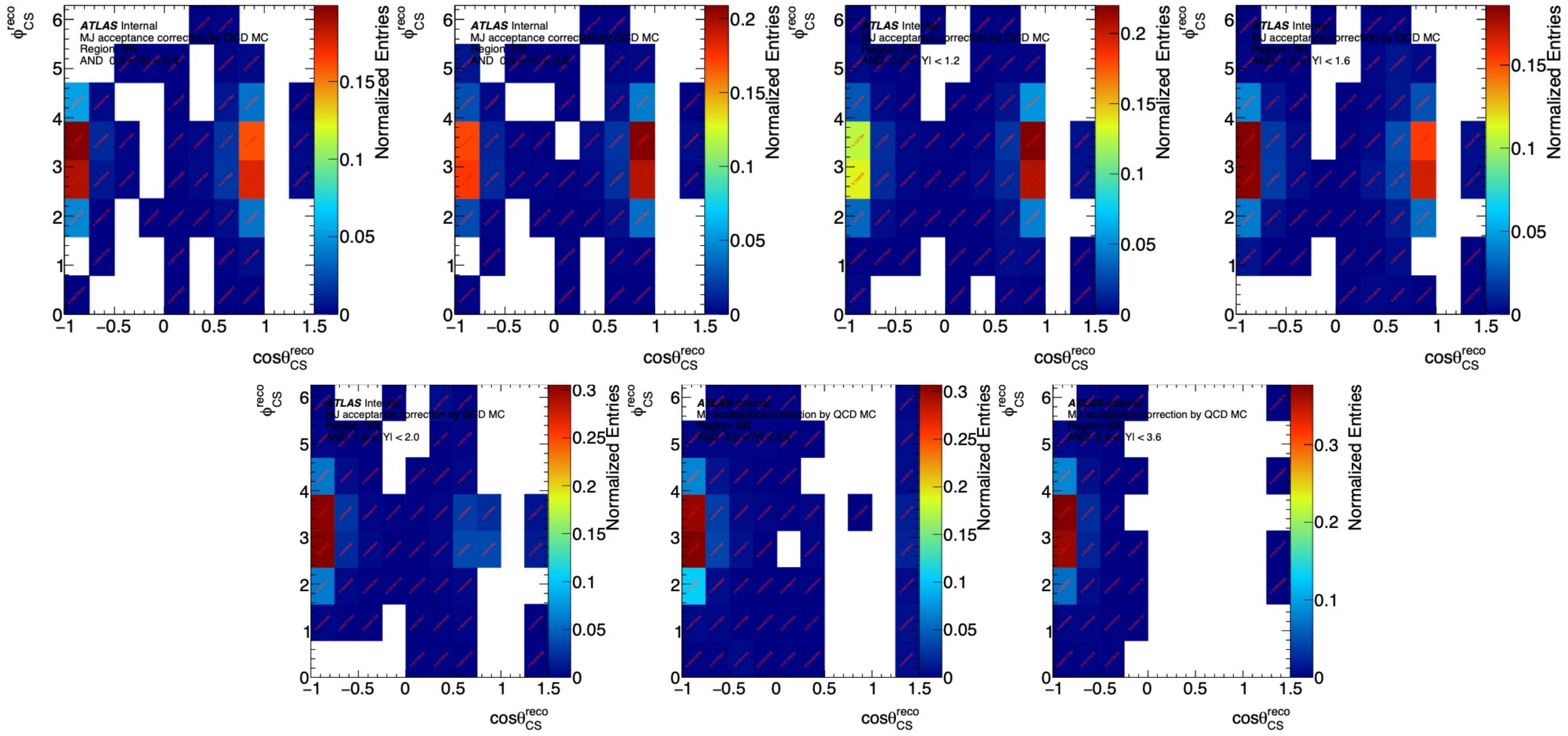

$|Y|$: [0, 0.4, 0.8, 1.2, 1.6, 2.0, 2.4, 3.6]

MJ templates for W-Ai analysis in $p_T^{l,\nu}$ binnning $W^- \to \mu^- \bar{\nu}$

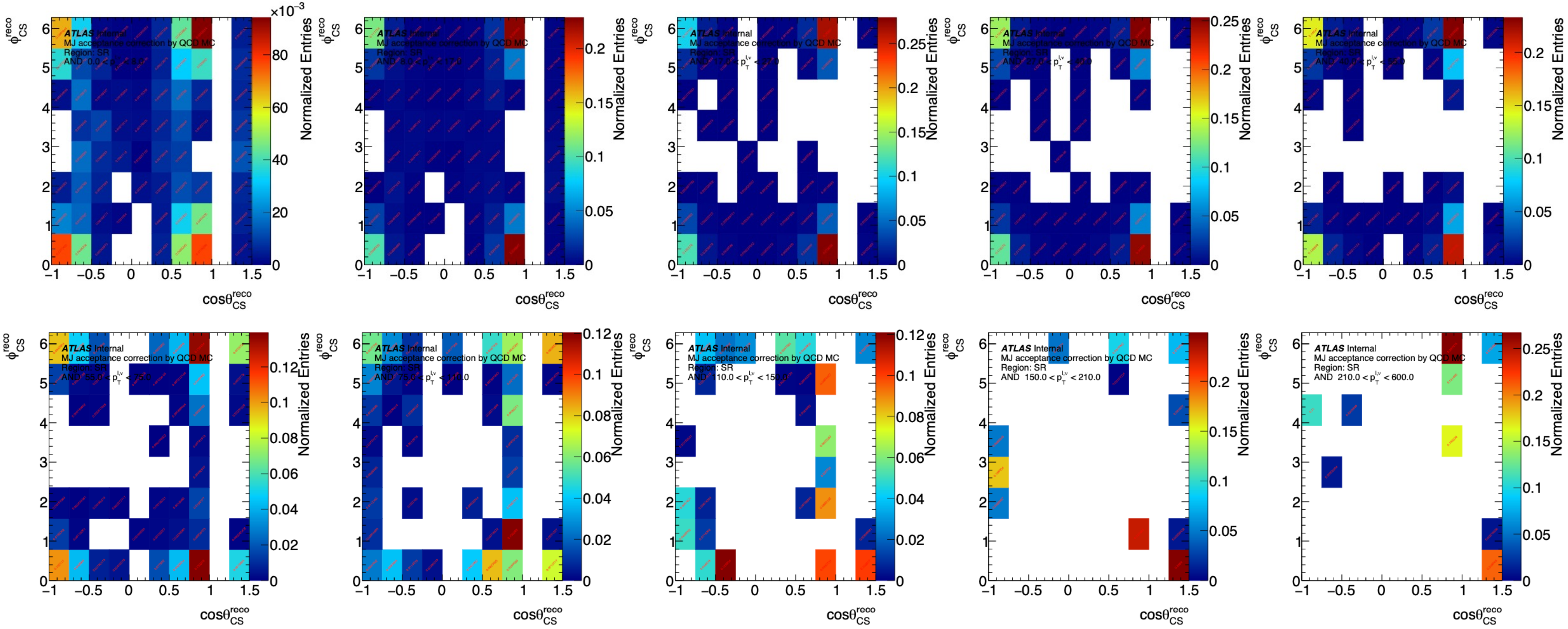

$$p_T^{\ell,\nu} : [0, 8, 17, 27, 40, 55, 75, 110, 150, 210, 600];$$

MJ templates for W-Ai analysis in $|Y|$ binnning $W^- \to \mu^- \bar{\nu}$

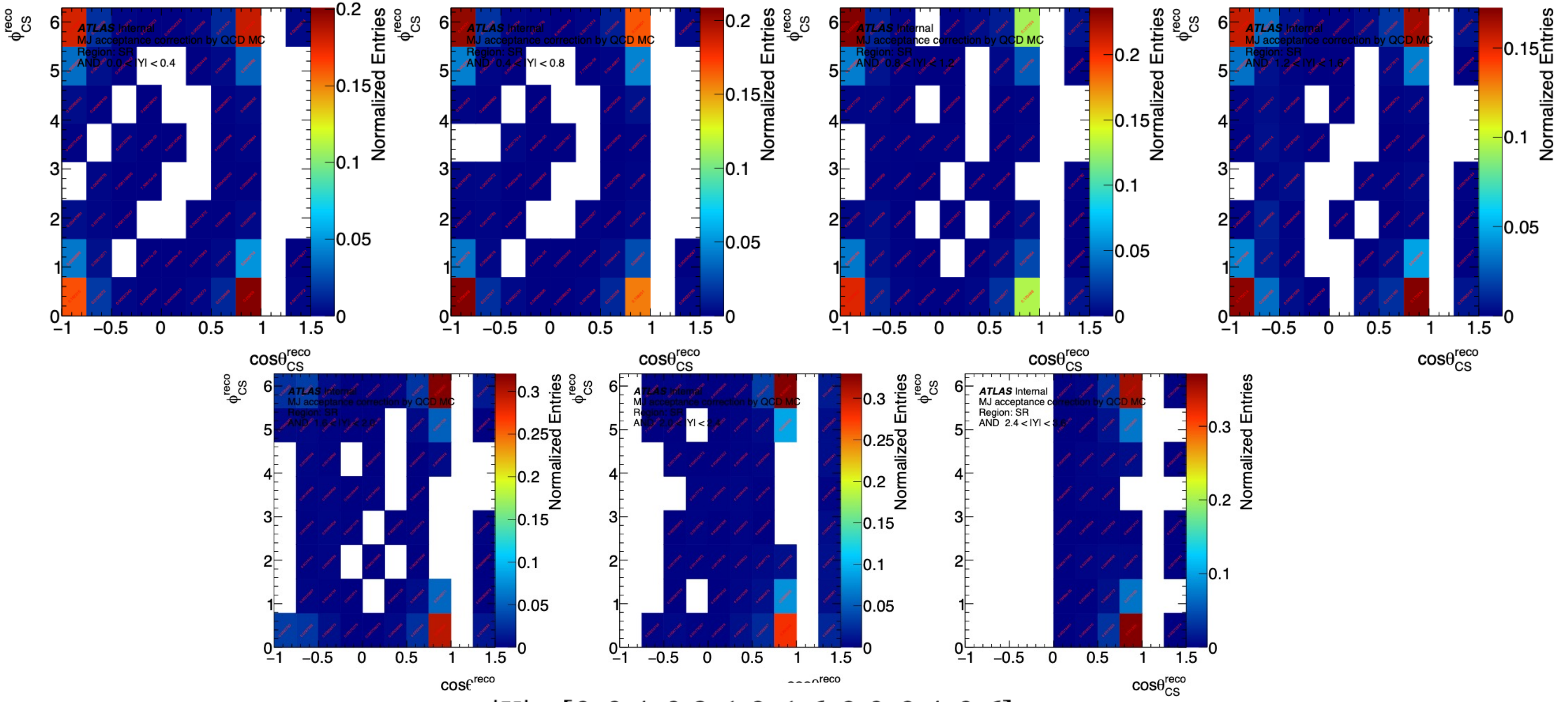

$|Y|$: [0, 0.4, 0.8, 1.2, 1.6, 2.0, 2.4, 3.6]

MJ systematics naming convention

Ludovica proposed a new naming convention.
Since xTR produces output for each p_T^W and Y^W bin, I dropping channel and bins numbering from the naming in the WS. Still, this naming convention should be easy to restore later in AiDY.

Name	# NP in AiDY	Comments
mj_yield_cor	1	MJ yield extrapolation (bin-by-bin correlated, two-sided).
mj_shape	3 for p_T^W / 3 for Y^W	MJ shape of the given $\cos\theta_{CS}$ :: ϕ_{CS} distribution in the coarse bin (bin-by bin uncorrelated, two-sided)
mj_acc_cor_closure	3 for p_T^W / 3 for Y^W	Apply difference between DD template and MC corrected template as acc corr sys uncertainty. This syst. is correlated within p_T^W and Y^W coarse bin. (bin-by-bin uncorrelated, **Q: two-sided?**)
mj_acc_cor_stat	10 for p_T^W / 7 for Y^W	Basically stat power of the QCD MC sample in the coarse and slicing bin used to fold MJ DD from coarse bin to the subregion. (bin-by-bin uncorrelated, two-sided)
mj_acc_cor_sys	10 for p_T^W / 7 for Y^W	Apply systematic as 100% on the acceptance correction it-slef. (bin-by-bin uncorrelated, **Q: two-sided?**)

Note: The "mj_yield_uncor" systematic is the MJ shape unc. in the SR for p_T^W (or Y^W) distribution. It affects yield normalisation in the given slice bin and it should be associated with 10 for p_T^W / 7 for Y^W NP. Impact of this syst. is huge, especially in the hard p_T^W region. We had agreed in July 2022 **not to use** "mj_yield_uncor" systematic in the fit.
Coarse bins: $p_T^{\ell,\nu}$: $0-17$ GeV, $17-55$ GeV, $55-600$ GeV; $|Y|$: $0-0.8$, $0.8-2.0$, $2.0-3.6$.

Systematic uncertainties breakdown

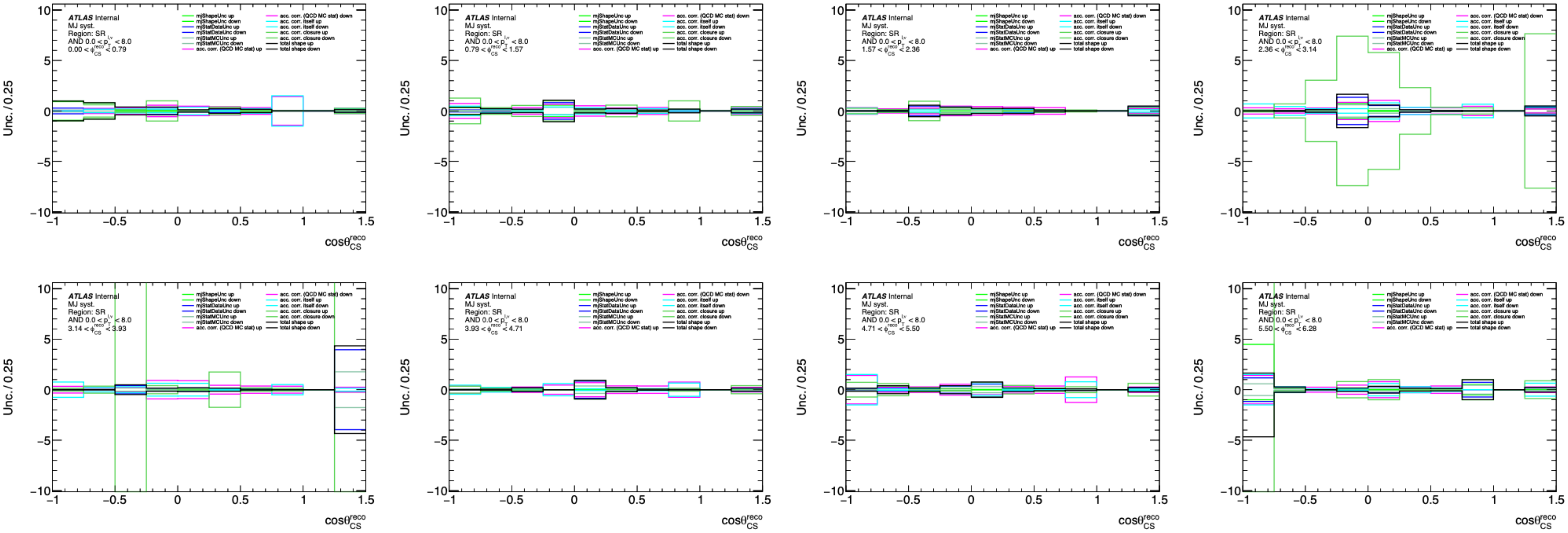

Figure 237: Multi-jet background shape systematics breakdown for $\cos\theta_{CS}$ as slices of ϕ_{CS} for $0 < p_T^{\ell,\nu} < 8$ GeV bin for $W^- \to e^-\overline{\nu}$ channel.

Systematic uncertainties breakdown

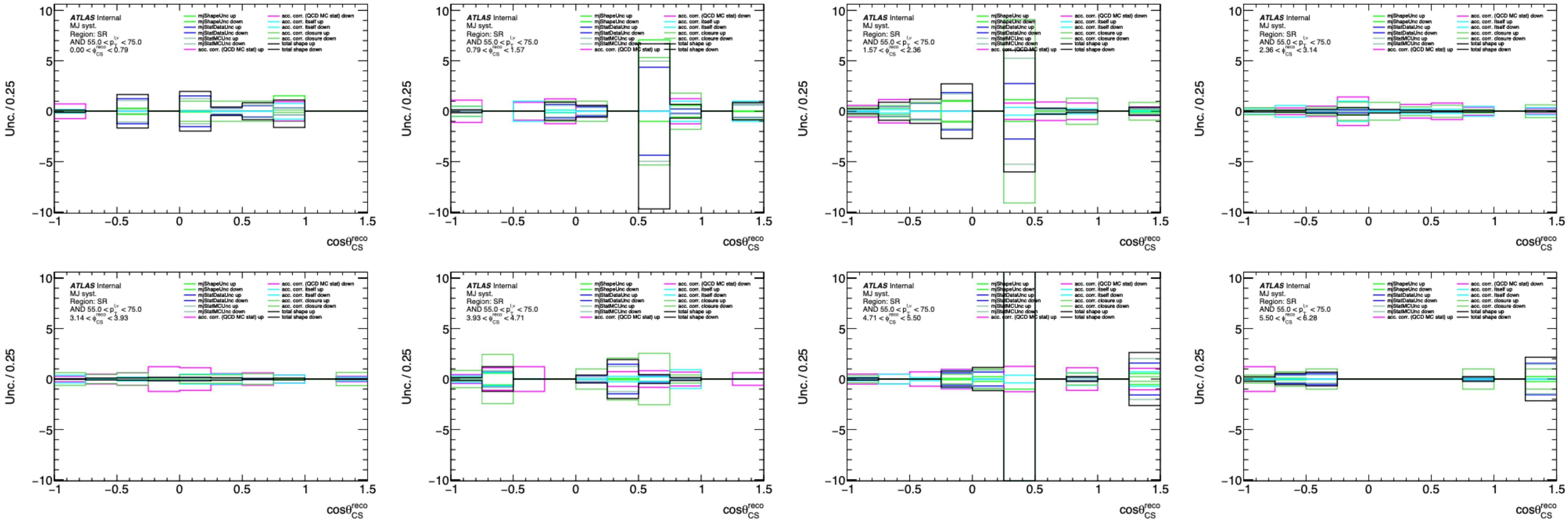

Figure 242: Multi-jet background shape systematics breakdown for $\cos\theta_{CS}$ as slices of ϕ_{CS} for $55 < p_T^{\ell,\nu} < 75$ GeV bin for $W^- \to e^-\overline{\nu}$ channel.

Systematic uncertainties breakdown

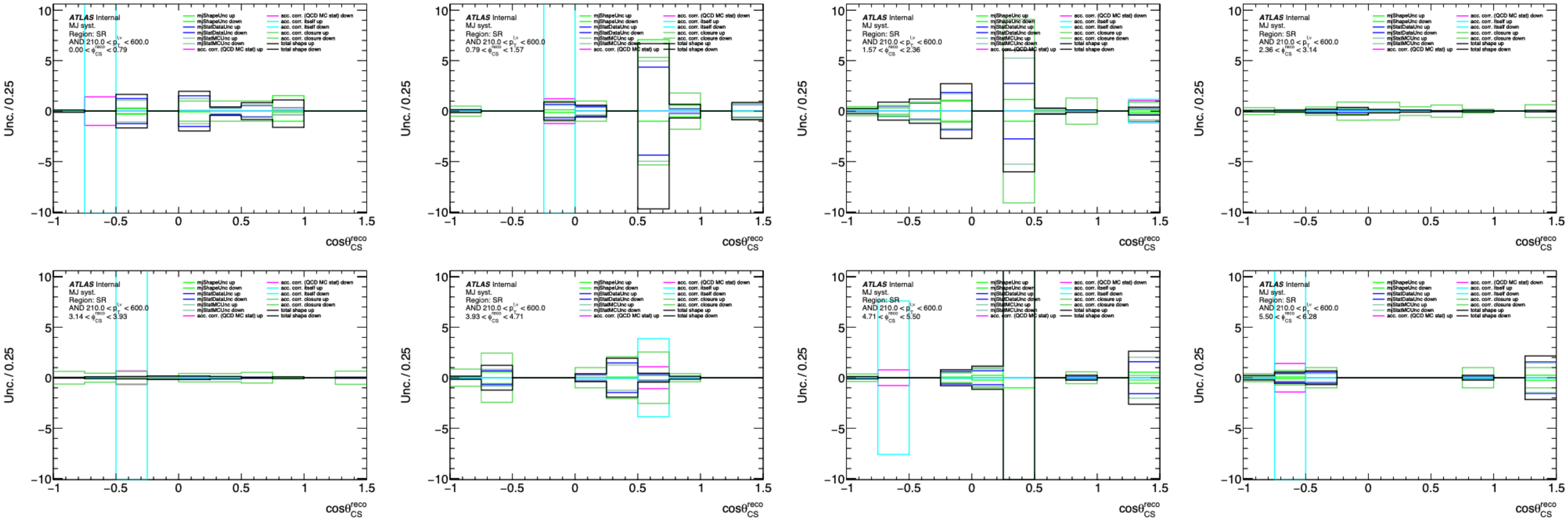

Figure 246: Multi-jet background shape systematics breakdown for $\cos\theta_{CS}$ as slices of ϕ_{CS} for $210 < p_T^{\ell,\nu} < 600$ GeV bin for $W^- \to e^-\bar{\nu}$ channel.

Ongoing tasks / problems

- Fit doesn’t work with real data (→Alex)
  - Works fine with Asmov and pseudo-data. For real data could not find minimum.
  - Perform cross-check using reco level only (Daniil)
    - Fit stability
    - MJ systematics constrains
- New NTuple production (→Daniil)
  - Apply new PTRW for pTW>100 GeV
  - Apply additional ID and iso SF systematics
  - Simplify systematics production
- PDF studies (→ Grigorii)
  - Theoretical predictions for multiple PDF sets and compare PDF uncertainties
    - CT10NLO, CT18NNLO, NNPDF4.0NNLO, MMHT20

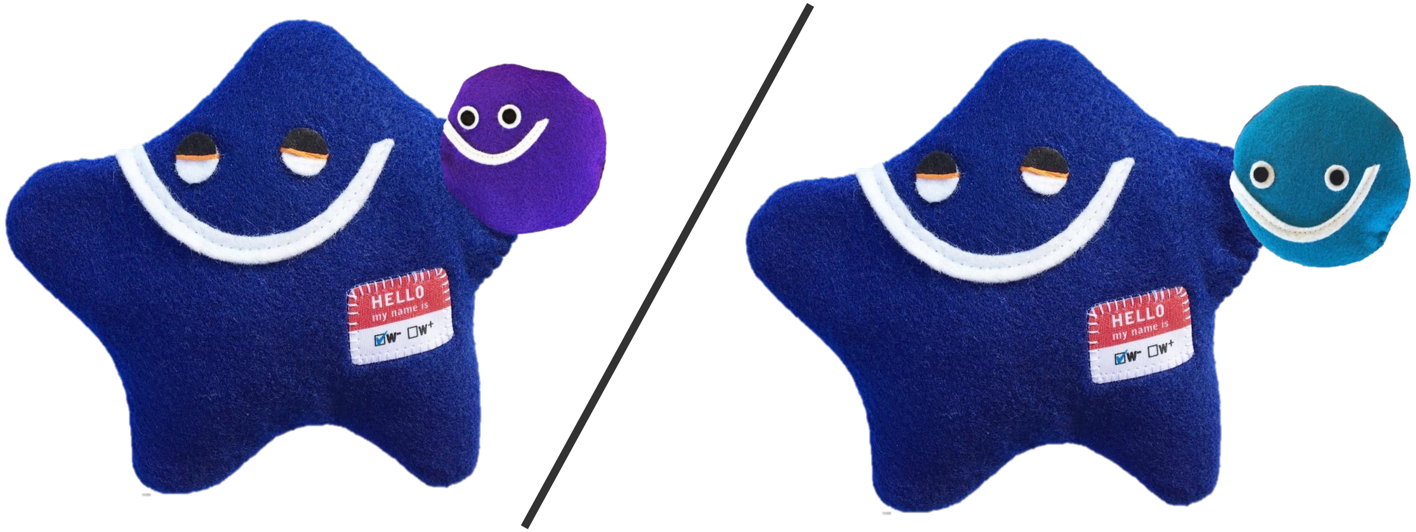

Thanks for attention!

Control Plots in the Signal Region for $W^+ \rightarrow e^+\nu$

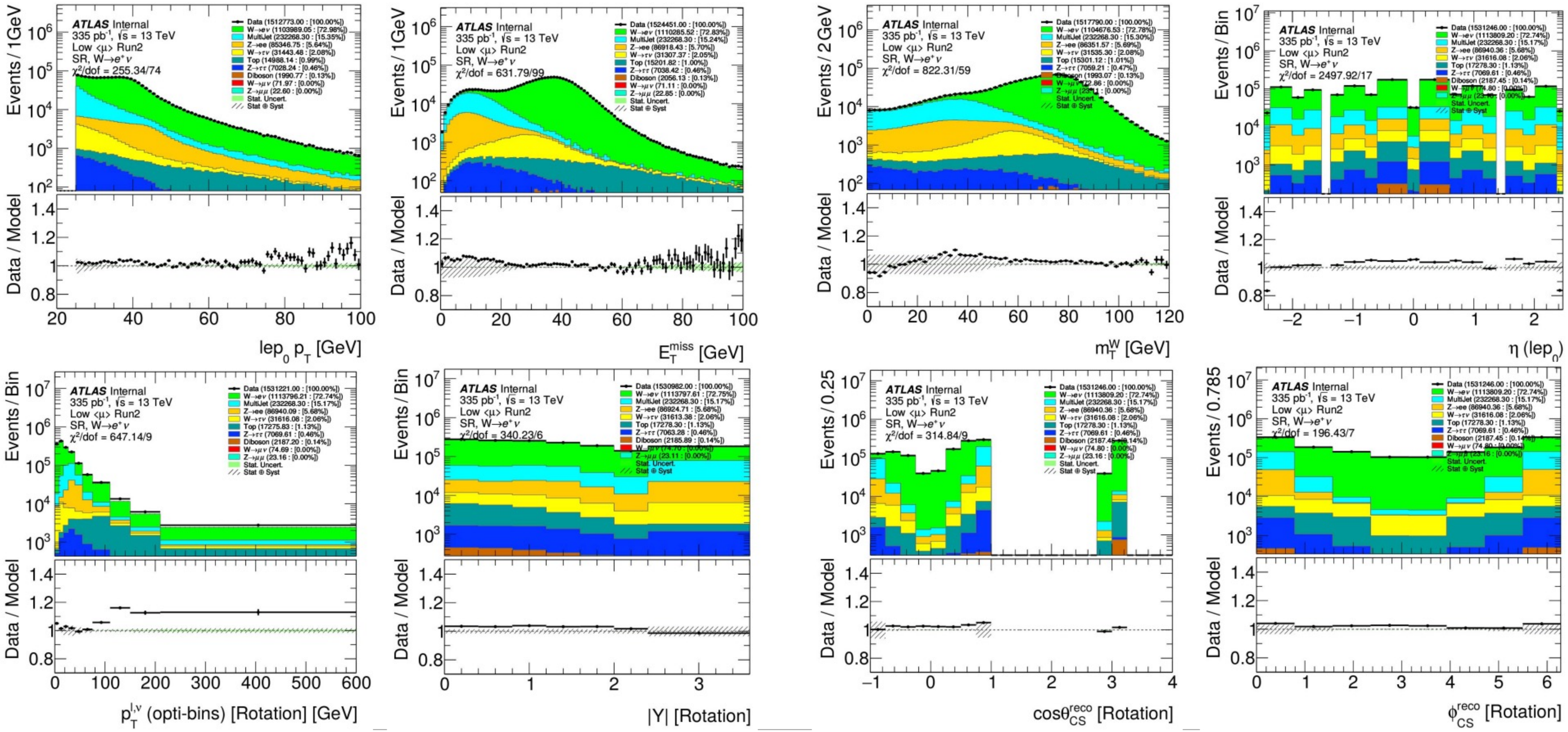

Control Plots in the Signal Region for $W^+ \rightarrow \mu^+\nu$

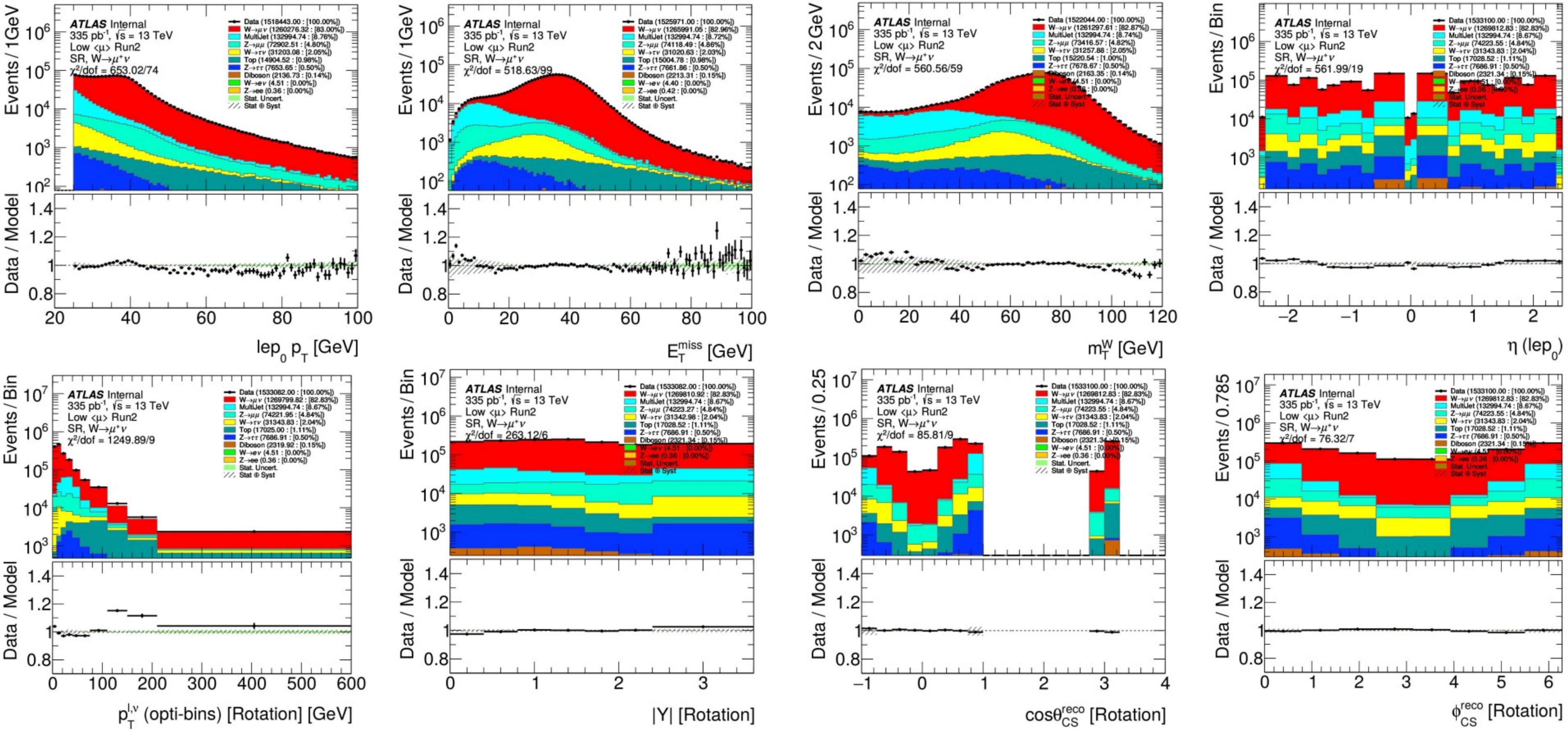

Collins Soper Frame

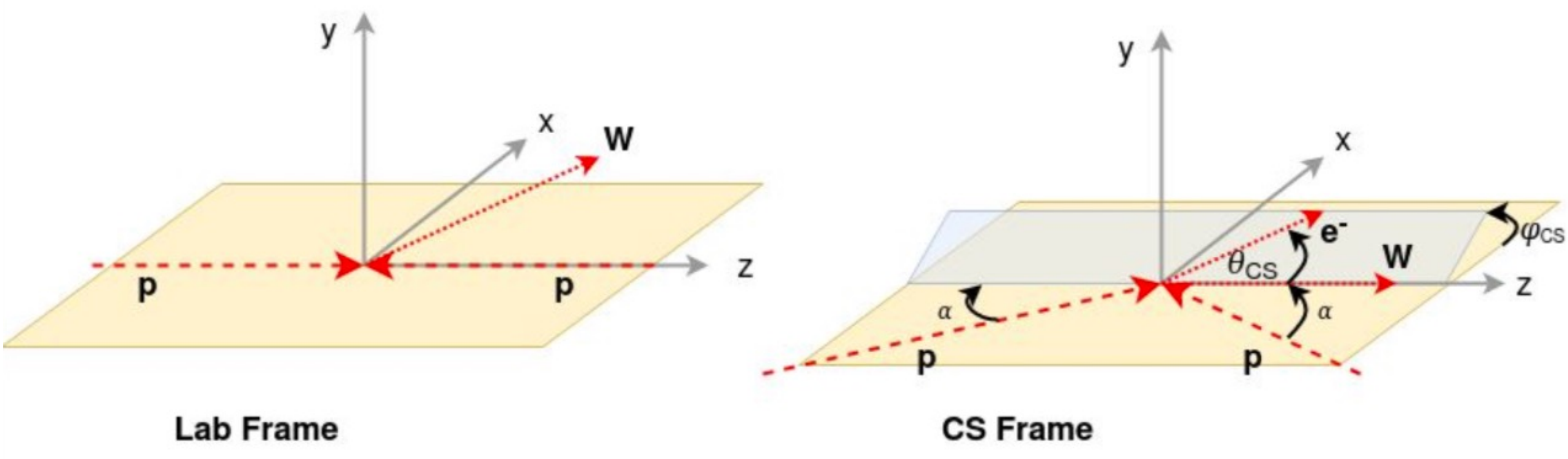

- Special W boson rest frame where angles are defined by lepton and proton kinematics.
- Define using "negative" lepton, so for W+ case this is the neutrino

Polynomial Information

$\mathbf{A_i}$	$\mathbf{P_i}$	$\mathbf{Y_l^m}(\theta, \phi)$	**Coupling**	**Non-Zero**
A_0	$1/2\left(1 - 3\cos^2\theta\right)$	Y_2^0		$\mathcal{O}\left(\alpha_S^1\right)$
A_1	$\sin 2\theta \cos\phi$	$\left(Y_2^{-1} - Y_2^1\right)$	$\left(v_\ell^2 + a_\ell^2\right)\left(v_q^2 + a_q^2\right)$	$\mathcal{O}\left(\alpha_S^1\right)$
A_2	$1/2\sin^2\theta\cos 2\phi$	$\left(Y_2^{-2} + Y_2^2\right)$		$\mathcal{O}\left(\alpha_S^1\right)$
A_3	$\sin\theta\cos\phi$	$\left(Y_1^{-1} - Y_1^1\right)$	$v_\ell a_\ell v_q a_q$	$\mathcal{O}\left(\alpha_S^1\right)$
A_4	$\cos\theta$	Y_1^0		$\mathcal{O}\left(\alpha_S^0\right)$
A_5	$\sin^2\theta\sin 2\phi$	$\left(Y_2^{-2} - Y_2^2\right)$	$\left(v_\ell^2 + a_\ell^2\right)\left(v_q a_q\right)$	$\mathcal{O}\left(\alpha_S^2\right)$
A_6	$\sin 2\theta\sin\phi$	$\left(Y_2^{-1} + Y_2^1\right)$		$\mathcal{O}\left(\alpha_S^2\right)$
A_7	$\sin\theta\sin\phi$	$\left(Y_1^{-1} + Y_1^1\right)$	$\left(v_\ell a_\ell\right)\left(v_q^2 + a_q^2\right)$	$\mathcal{O}\left(\alpha_S^2\right)$

Physics Modelling

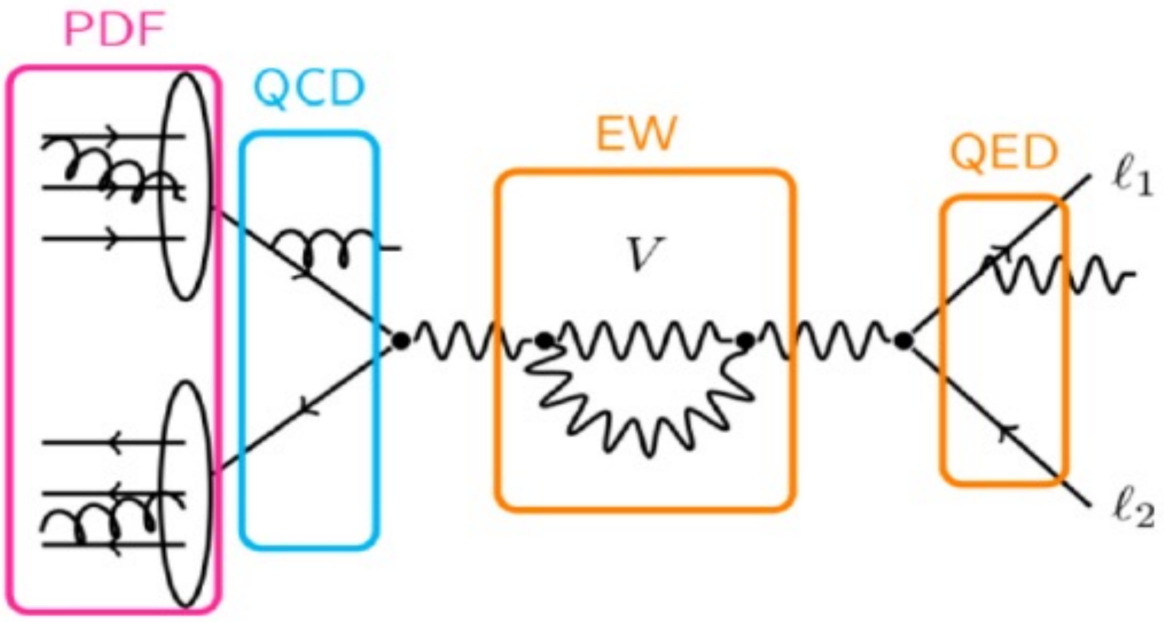

Angular Coefficients

$$\frac{d\sigma}{dp_T^W\, dm^W\, dy^W\, d\cos\theta\, d\phi} = \frac{3}{16\pi}\frac{d\sigma^{U+L}}{dp_T^W\, dm^W\, dy^W}\Big\{(1+\cos^2\theta) + \frac{1}{2}A_0(1-3\cos^2\theta)$$
$$+ A_1 \sin 2\theta\cos\phi + \frac{1}{2}A_2\sin^2\theta\cos 2\phi$$
$$+ A_3\sin\theta\cos\phi + A_4\cos\theta + A_5\sin^2\theta\sin 2\phi$$
$$+ A_6\sin 2\theta\sin\phi + A_7\sin\theta\sin\phi\Big\}.$$

Non-zero at LO

Non-zero at NLO

Non-zero at NNLO

- Full angular cross-section parameterization
- QCD production dynamics fully contained in Ai coefficients, while decay kinematics fully contained in coupled angular polynomials

Neutrino reconstruction

- Angular definitions require fully constructed neutrino
- Hadronic recoil:
  - Vectorial sum of all transverse momenta of ISR objects
  - ATLAS: uses PFlow objects (neutral+charged)
- Solving for Neutrino p_z:
  - Take mass constraint resulting in quadratic equation
    - $(q_l + q_\nu)^\mu \, (q_l + q_\nu)_\mu = m_W^2$
  - $m_T < m_W$ gives 2 solutions
    - one chosen at random but can statistically resolve correct distributions
  - No real solution when $m_T > m_W$, still can use events for φ_{CS} information
- Once the mass constraint is chosen φ_{CS} is solved while the 2 solutions corresponds to a sign ambiguity in $\cos\theta_{CS}$

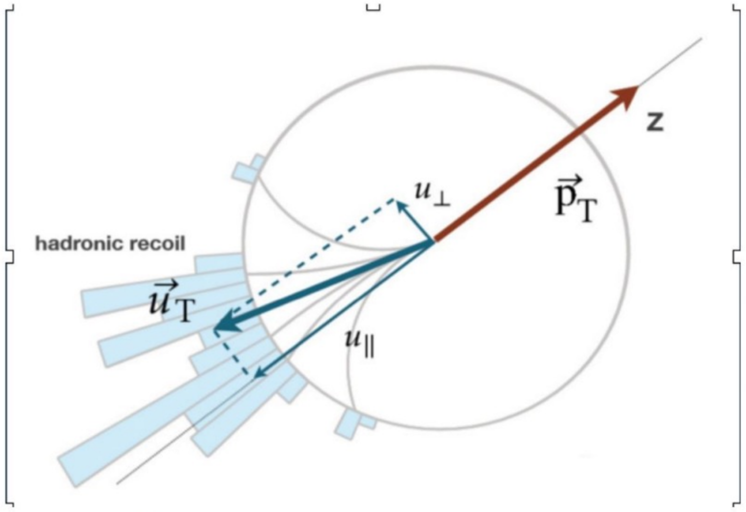

$$\vec{E}_T^{miss} = \vec{p_T}^{\nu} = -\left(\vec{u_T} + \vec{p_T}^{\ell}\right)$$

$cos\theta_{CS}$ ambiguity (1)

More info

- How can we statistically resolve $cos\theta_{CS}$?

$$\cos\theta = 2\frac{(l^+\bar{l}^- - l^-\bar{l}^+)\cdot \text{sign}(y_{\ell\ell})}{m_{\ell\ell}\sqrt{m_{\ell\ell}^2 + \vec{p}_T^{\,2}}},$$

$l^{\pm} = E \pm p_z$ for the lepton/neutrino
$\bar{l}^{\pm} = E \pm p_z$ for the antilepton/antineutrino

- Only choose correct p_z 50% of the time, incorrect p_z can still be used

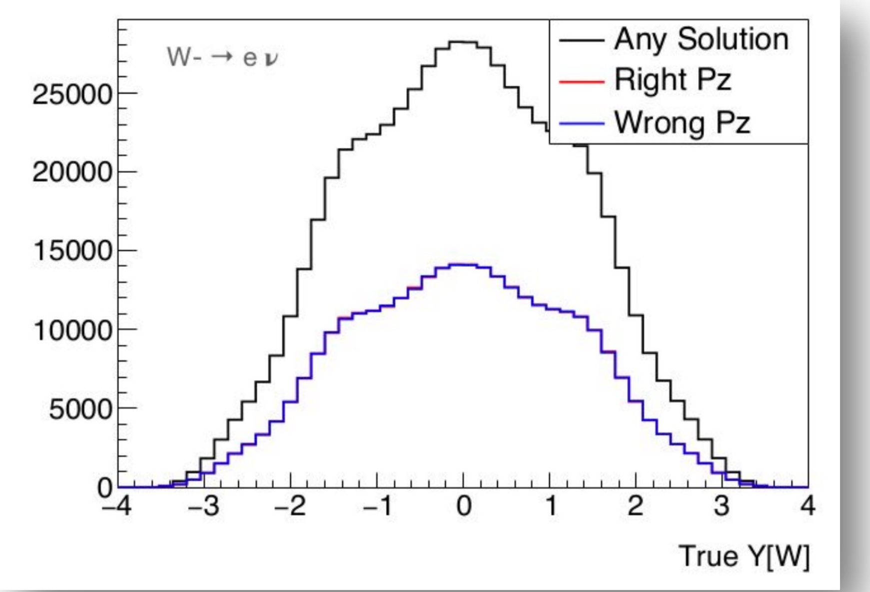

- Can solve it in 2 cases:
  - 1) Solutions where y_{ll}^1 and y_{ll}^2 have opposite signs
    - sign flips in orange and blue cancel
  - 2) One of the solutions violates Bjorken condition x < 1
    - neutrino has more p_z than beam energy → unphysical

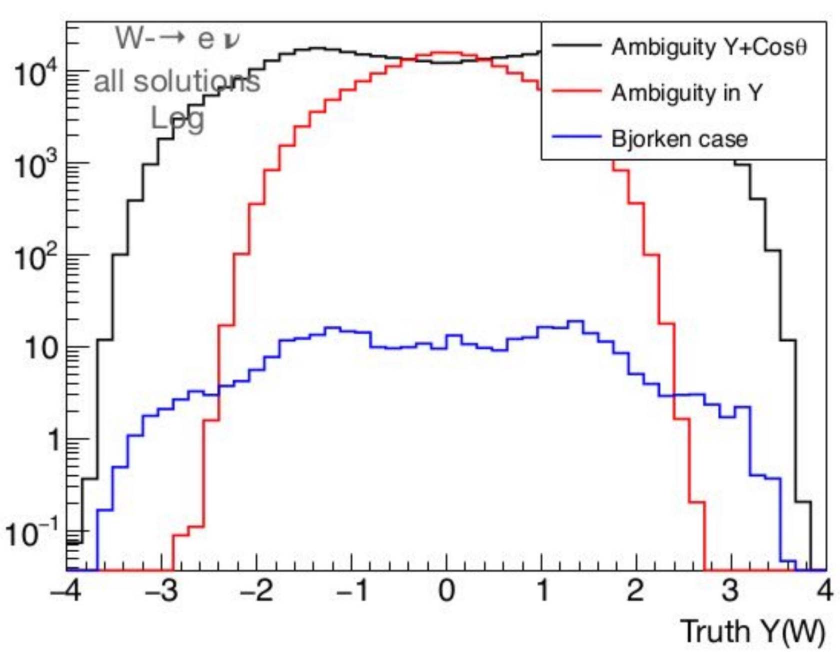

$\cos\theta_{CS}$ ambiguity (2)

- Red are events where we picked right p_z to get right sign of $\cos\theta_{CS}$
- Green are events where we picked wrong p_z but y_{ll} flipped so we get correct $\cos\theta_{CS}$, these are the events where we get our sensitivity.

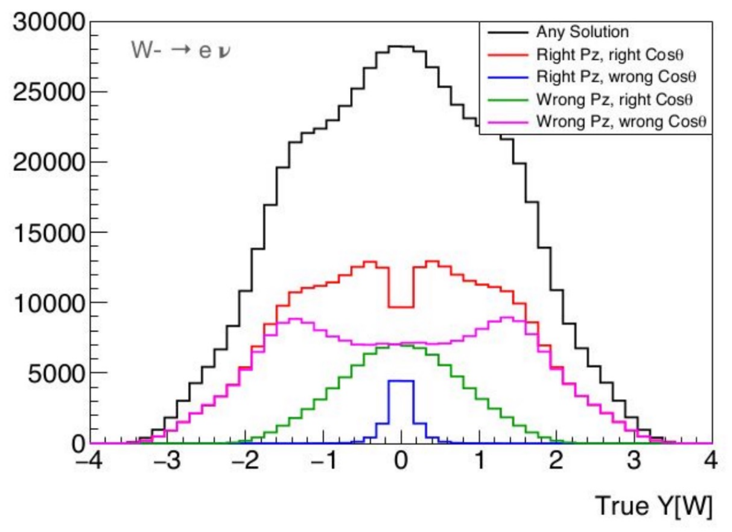

1) Both $\cos\theta_{CS}$ and y_{ll} have sign ambiguity so right 50%, no A_4 sensitivity

2) Adding to 1): only y^W has ambiguity which cancels with $\cos\theta_{CS}$ → right 100% (where we gain our sensitivity)

3] Adding to 2): One solution doesn't satisfy Bjorken condition (x < 1) → right 100% but pretty rare

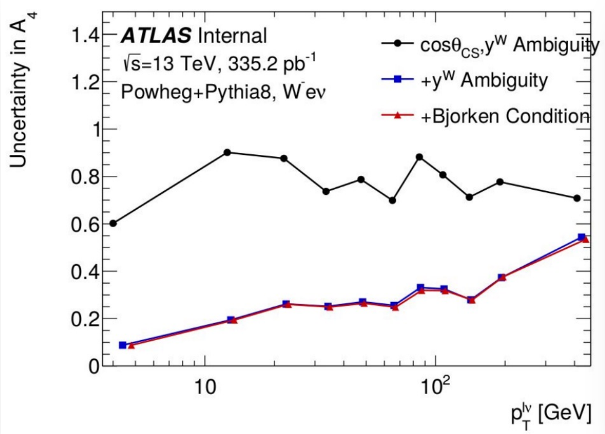

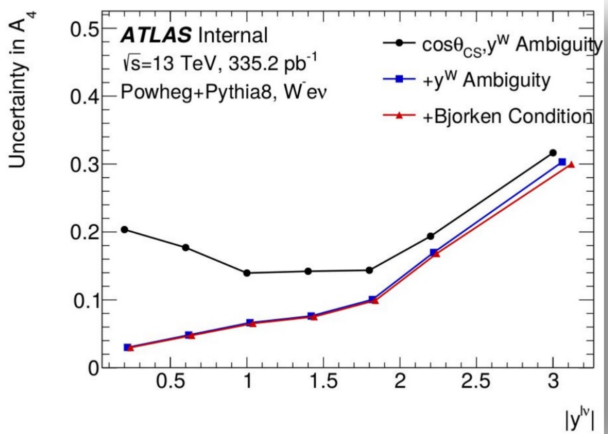

Top Background (1)

When first adding background, the increase in uncertainty was larger than expected especially at high $p_T^{l,\nu}$.

Due to larger top background contributions.

Preliminarily we thought a $|\Delta\phi| > \pi/4$ cut should help reduce the top background but doesn't as shown on the next slide.

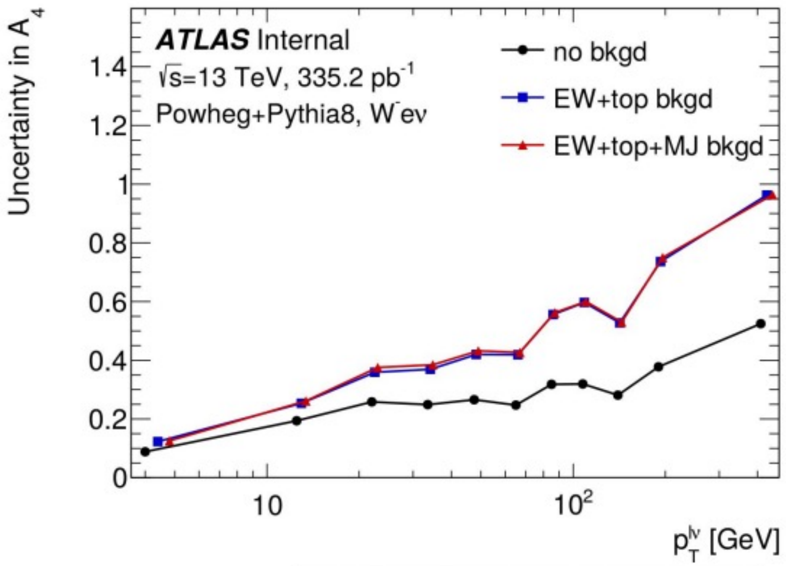

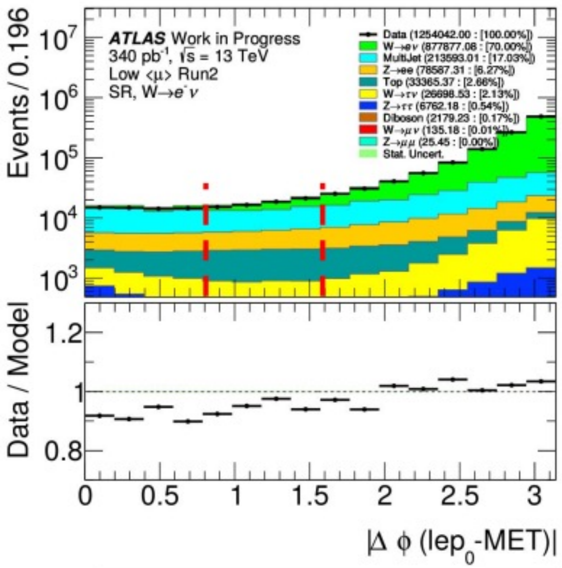

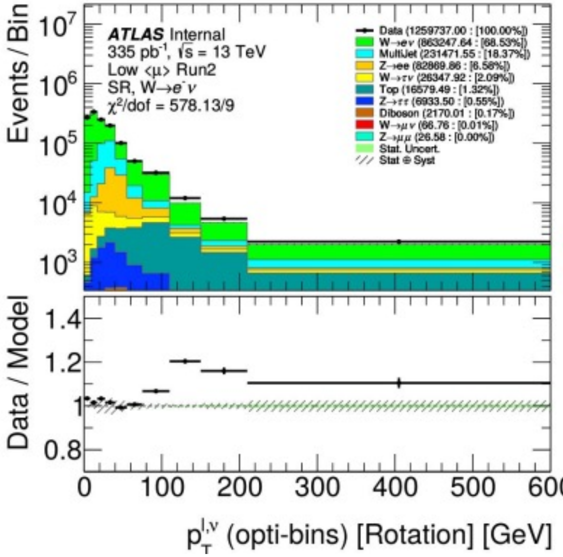

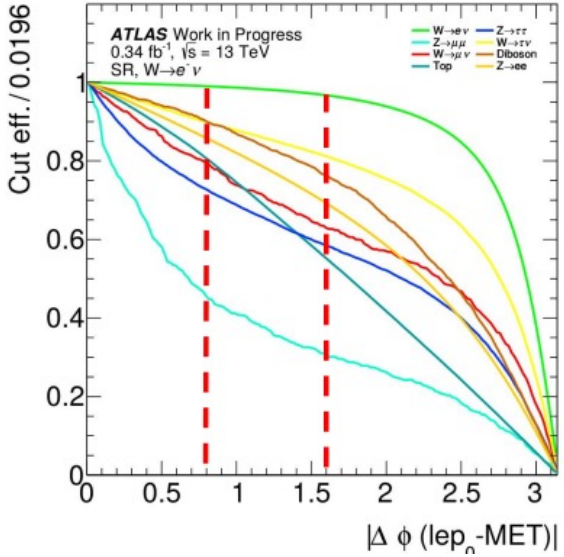

Top Background (2)

Both signal and background at high p_T lose all $\cos\theta_{CS}$ shape information and causing large uncertainty.

Addition of MET cut reduces background but also signal too much.

From our studies the top background seems irreducible.

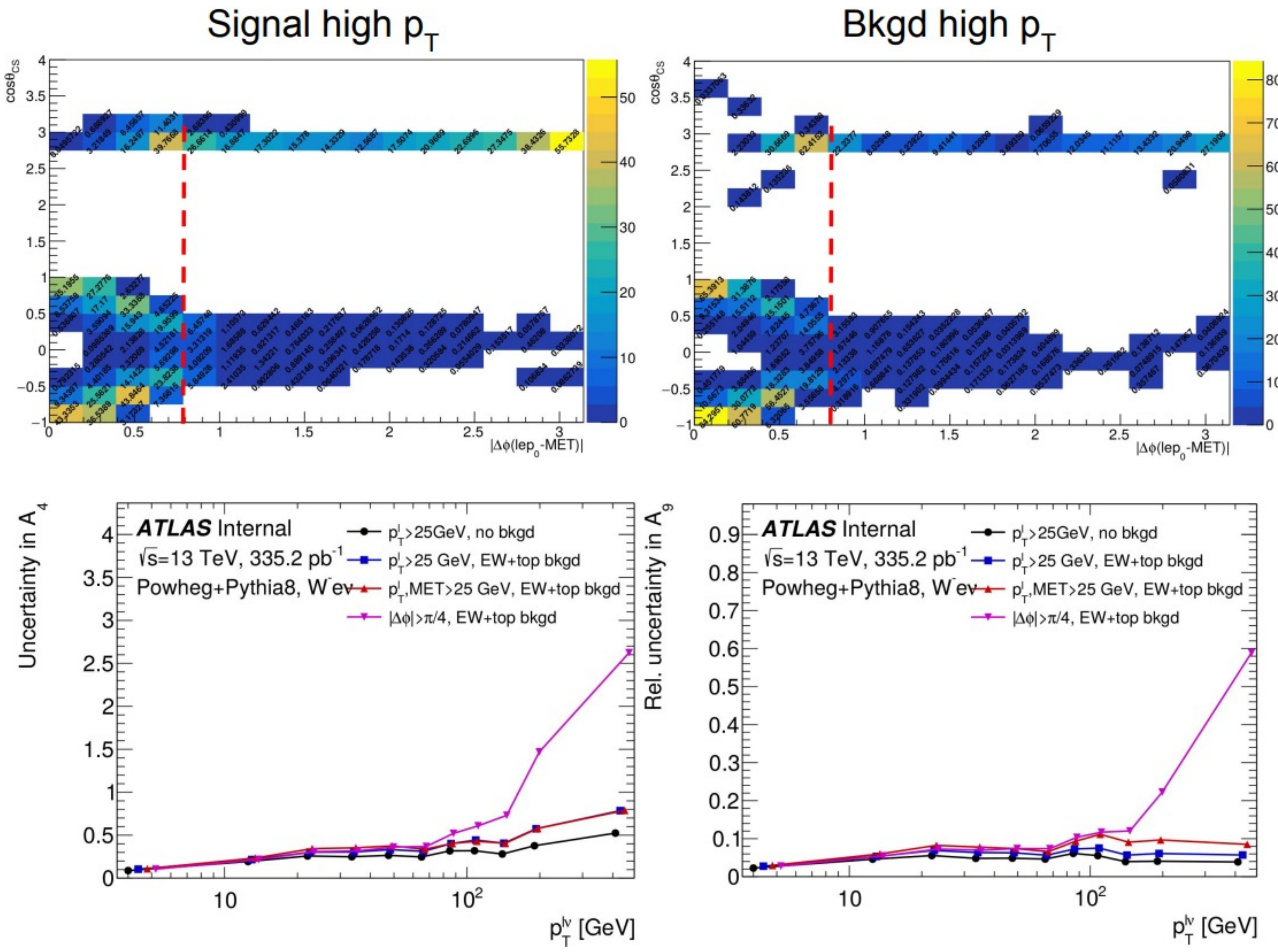

Event selection: Sensitivity Comparison

A_0

A_4

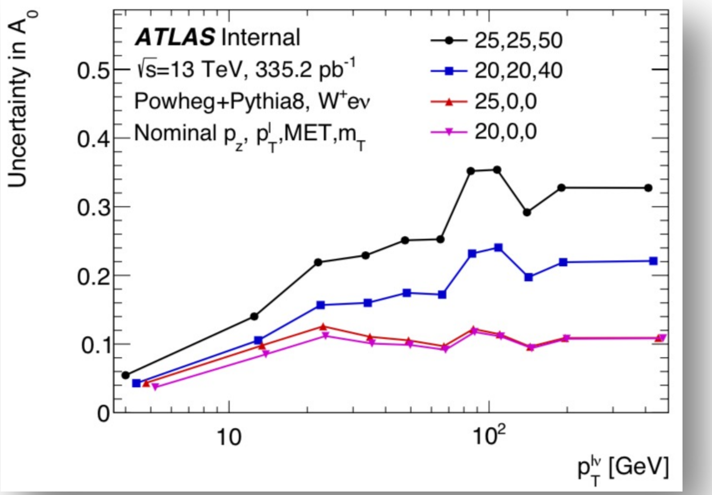

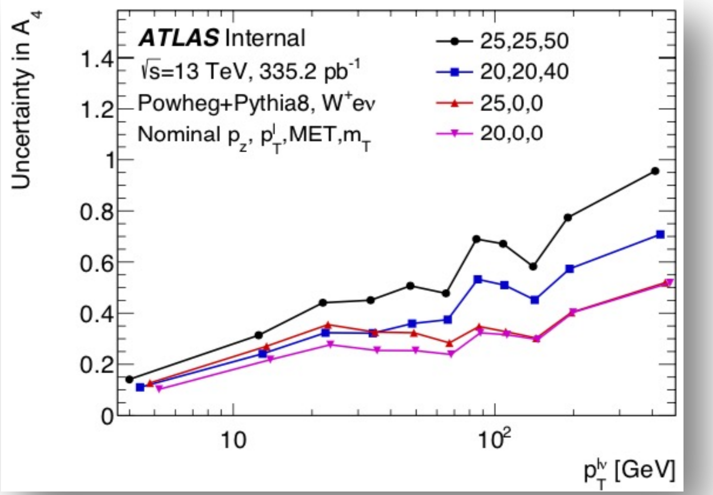

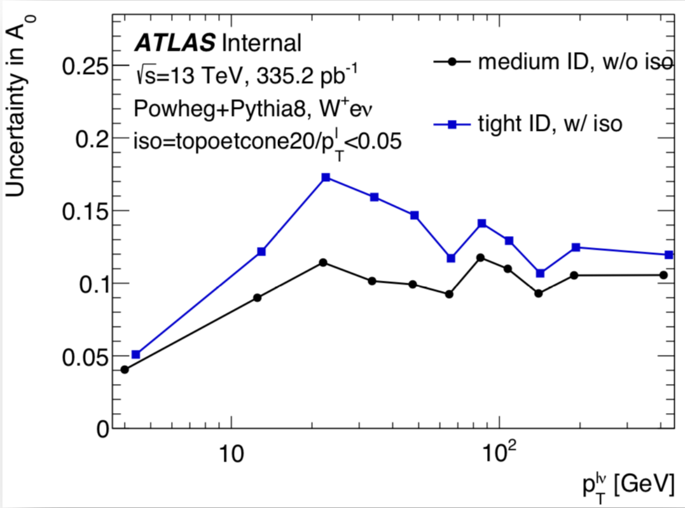

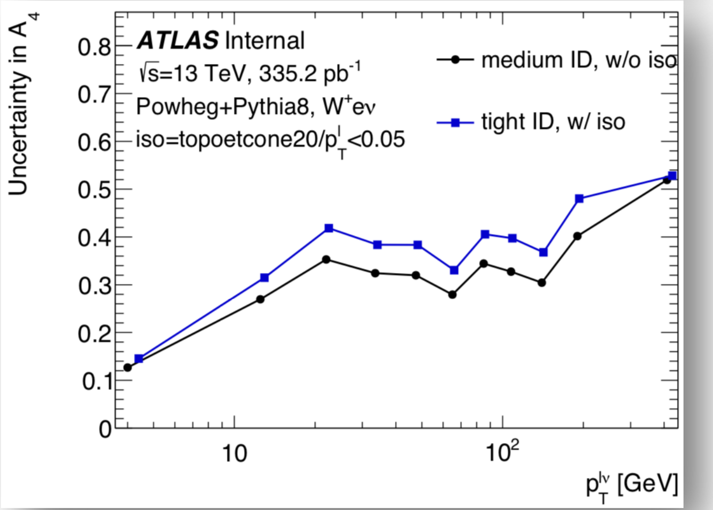

Systematics

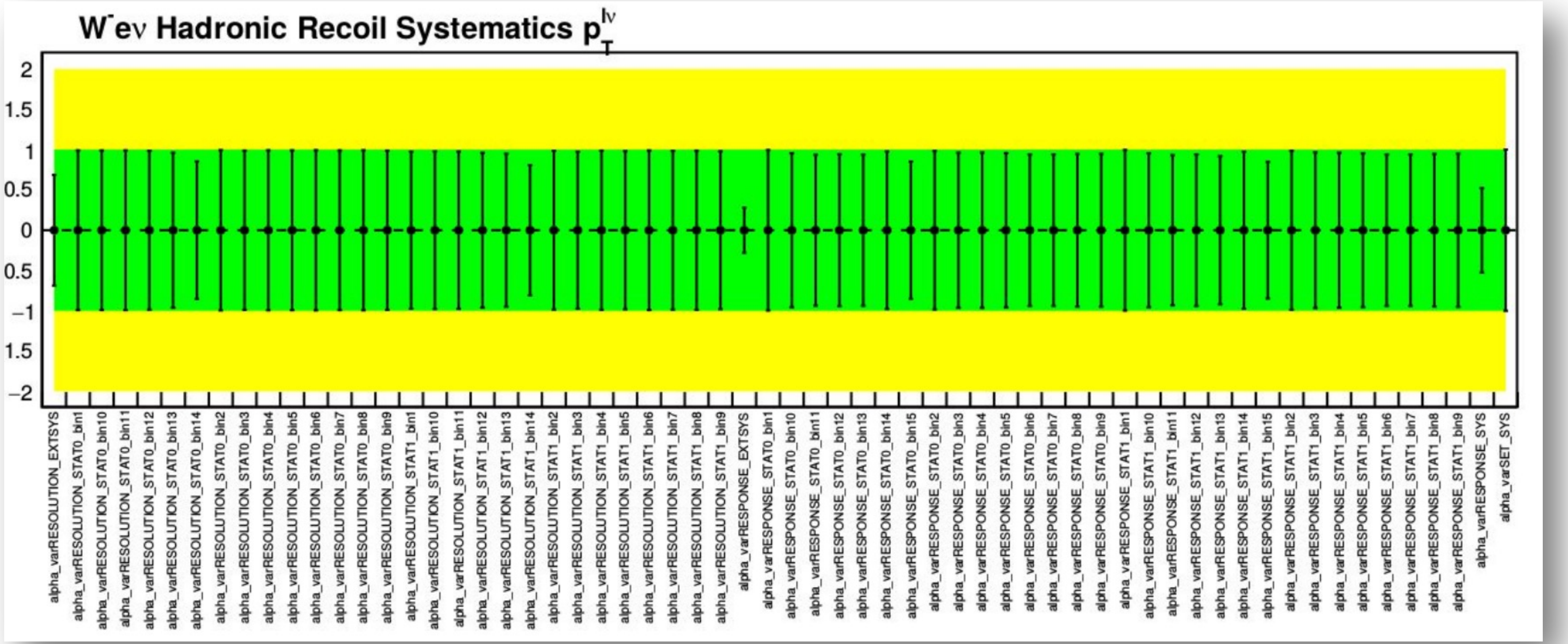

- Have tested 2 largest expected systematics (Hadronic Recoil and Background) independently
- MJ NPs heavily constrained, still being understood.

MJ Acceptance Systematic (8 < pT < 17 GeV)

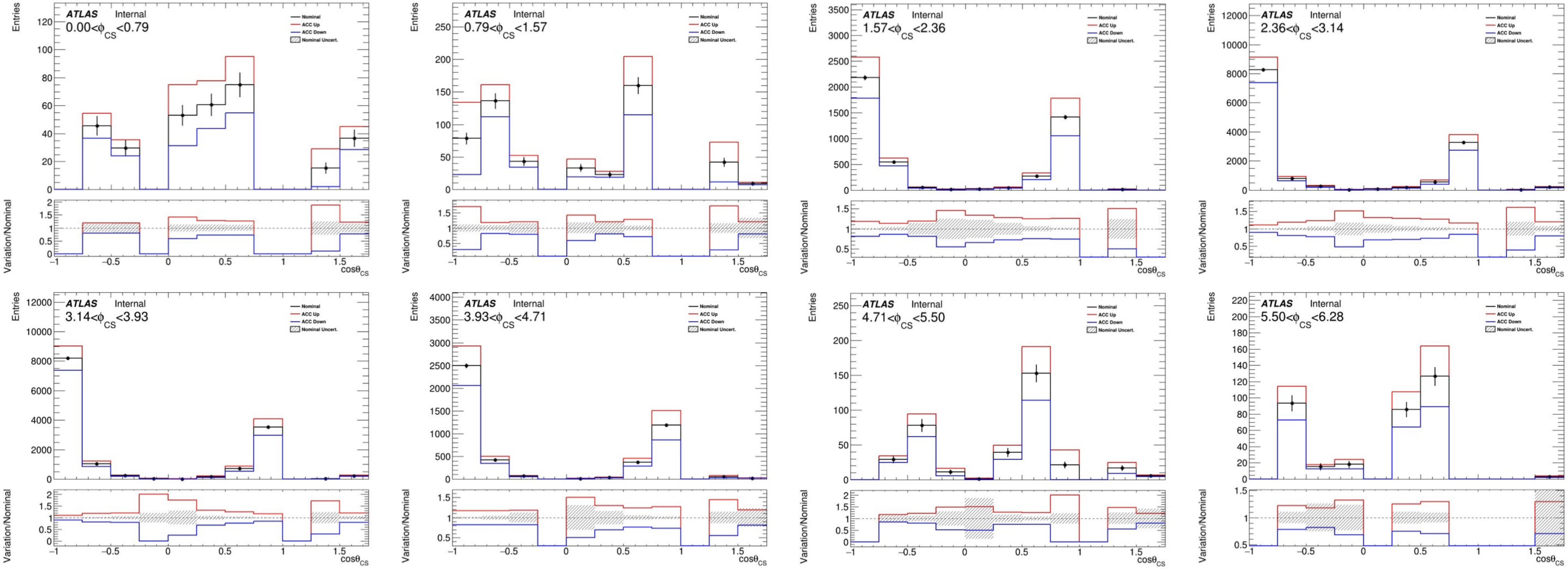

MJ Shape Systematic (8 < pT < 17 GeV)

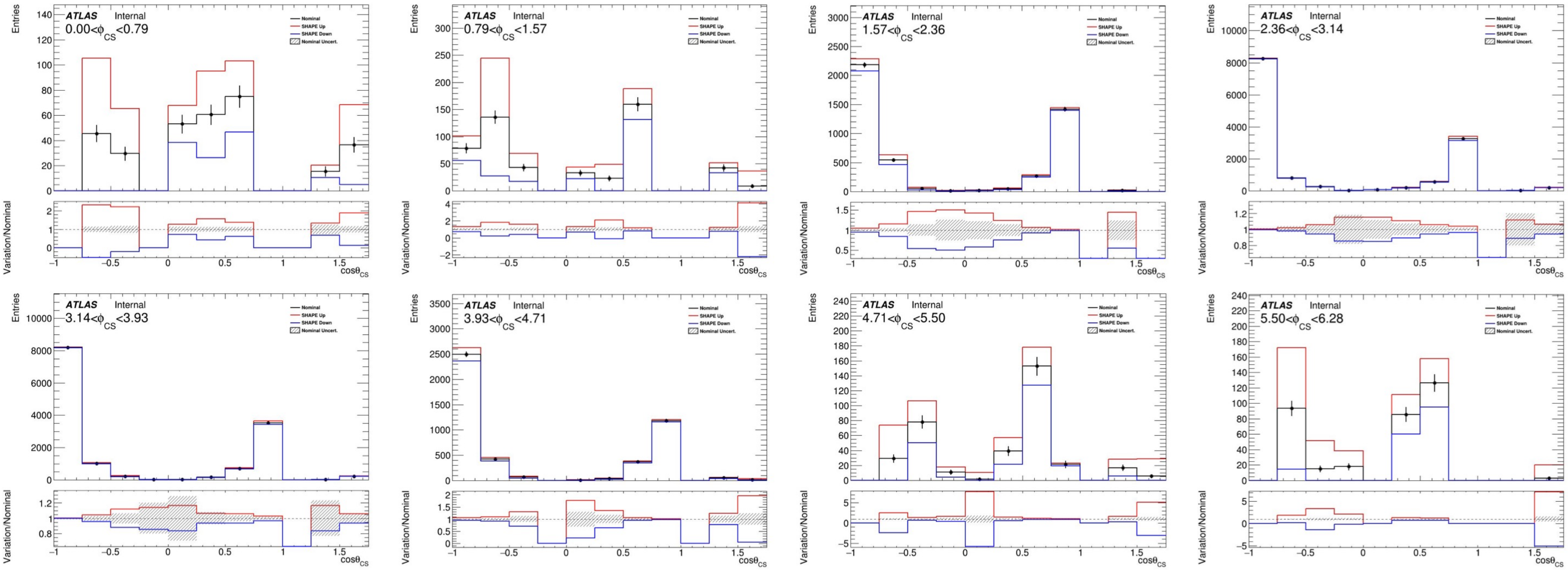

MJ templates derived for pure DD and predicted by QCD MC

$W \to e^{-}\nu$

$W \to \mu^{-}\nu$

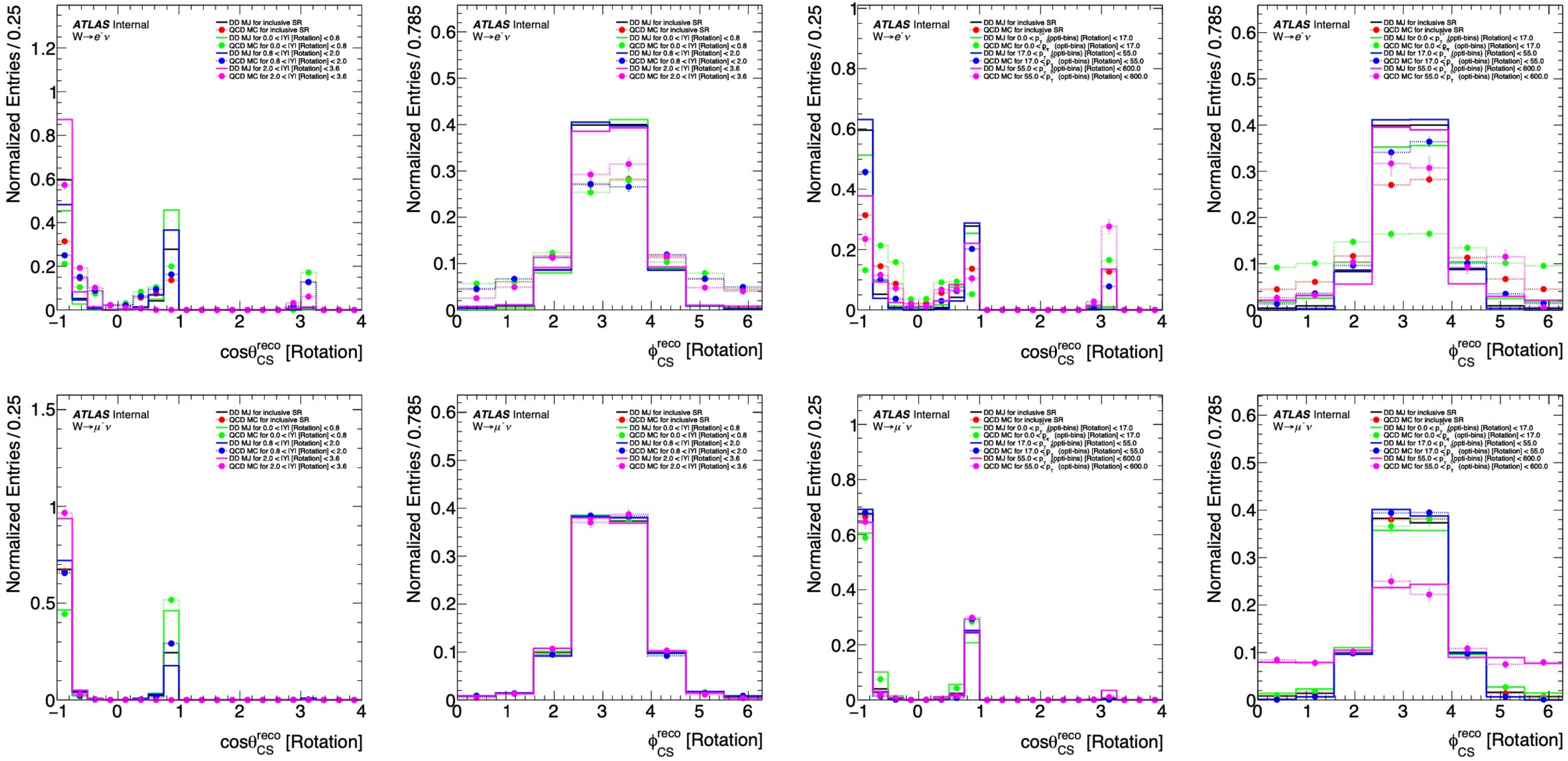

Debugging: MJ templates derived by accCorr

$W \to e^- \nu$

$W \to \mu^- \nu$

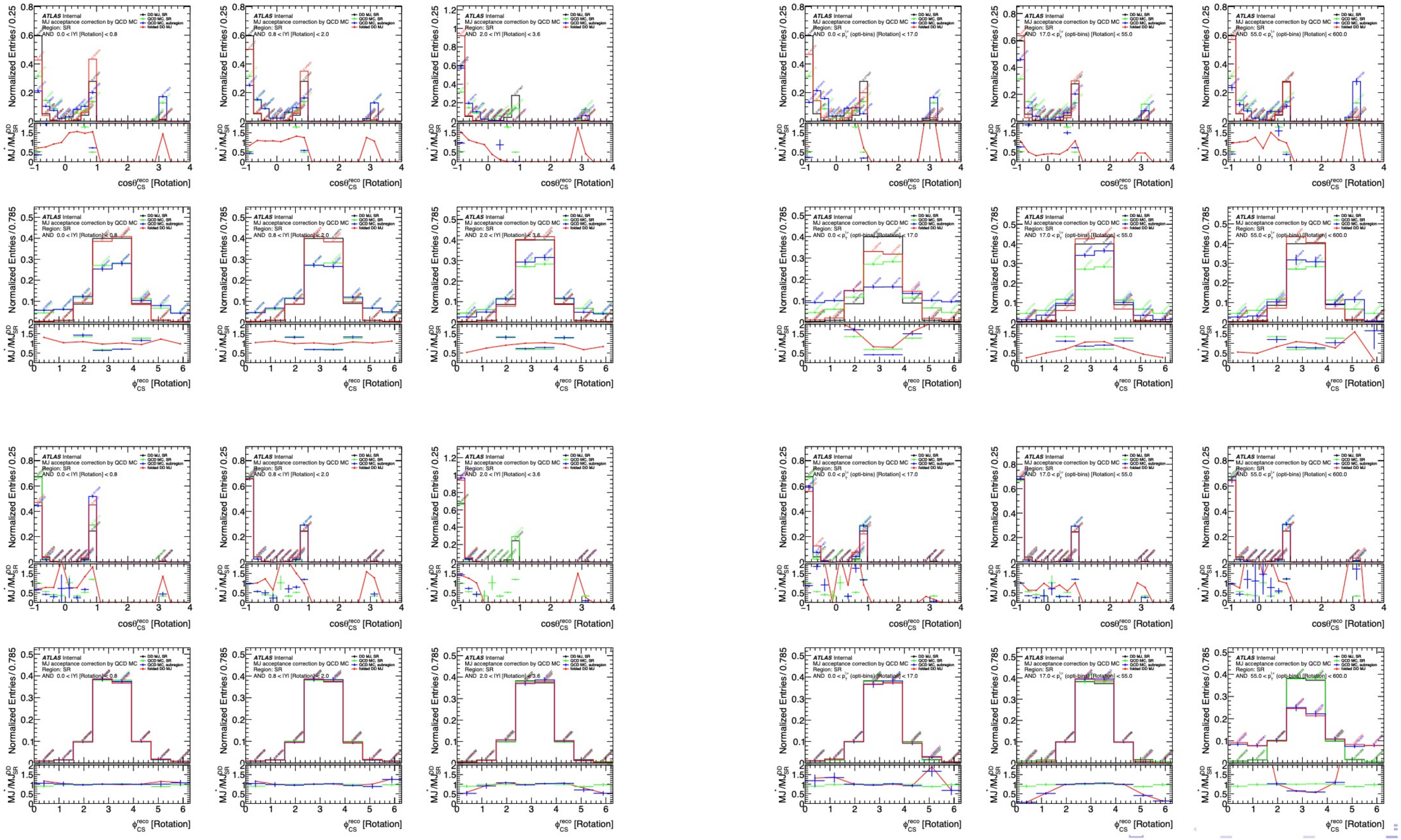

Debugging: accCorr functions

$W \to e^- \nu$

$W \to \mu^- \nu$

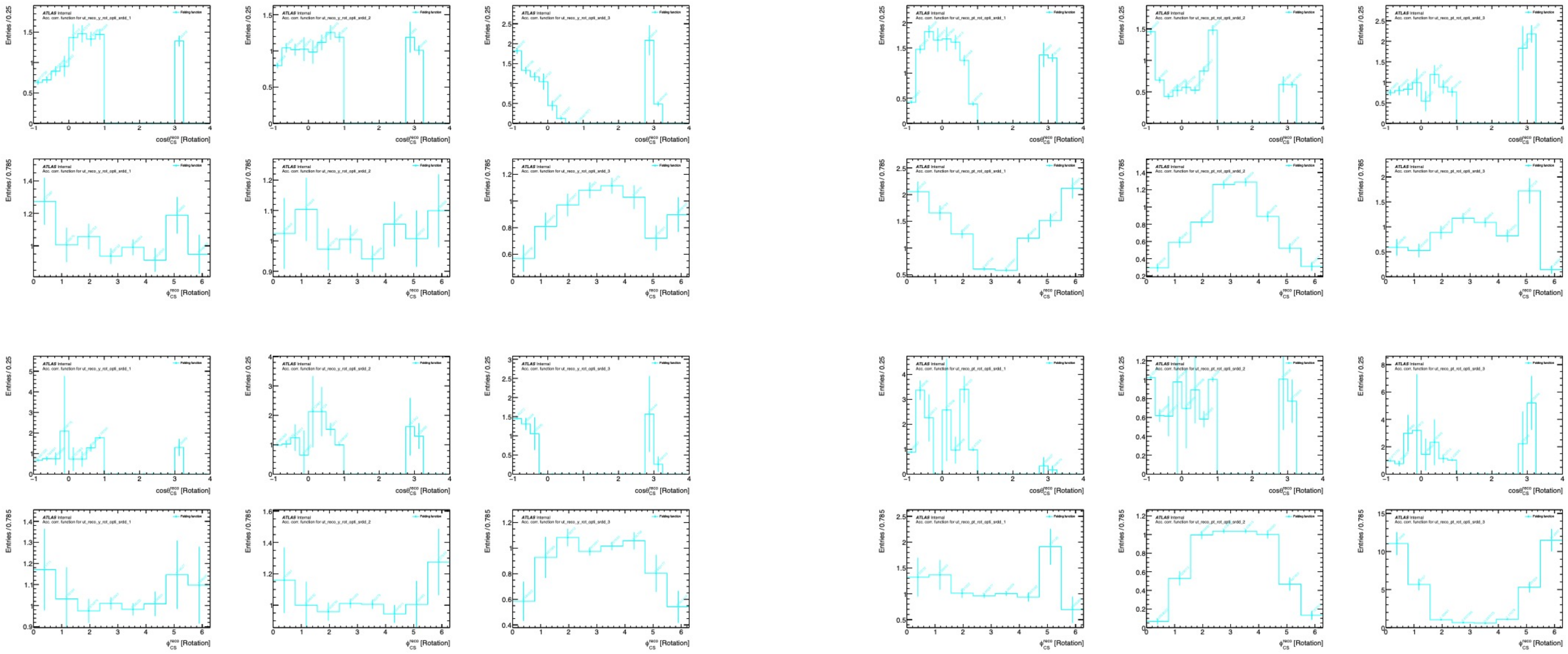

Acc Correction for 3D templates

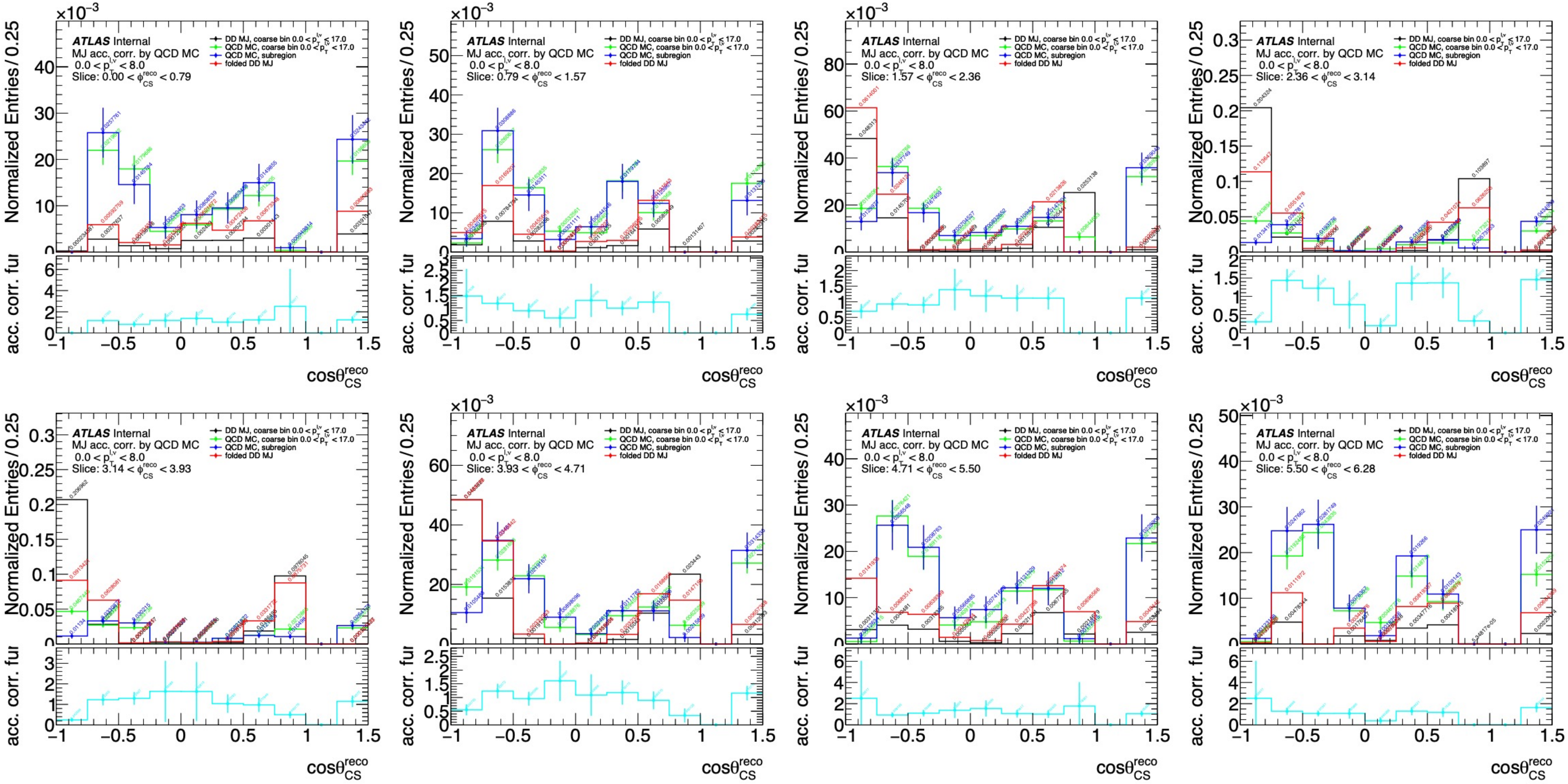

Figure 161: Multi-jet background template acceptance correction functions for $\cos\theta_{CS}$ as slices of ϕ_{CS} for $0 < p_T^{\ell,\nu} < 8$ GeV bin for $W^- \to e^-\bar{\nu}$ channel. Distributions are normalized over ϕ_{CS} slices. Error bands represents statistical uncertainties.

Acc Correction for 3D templates

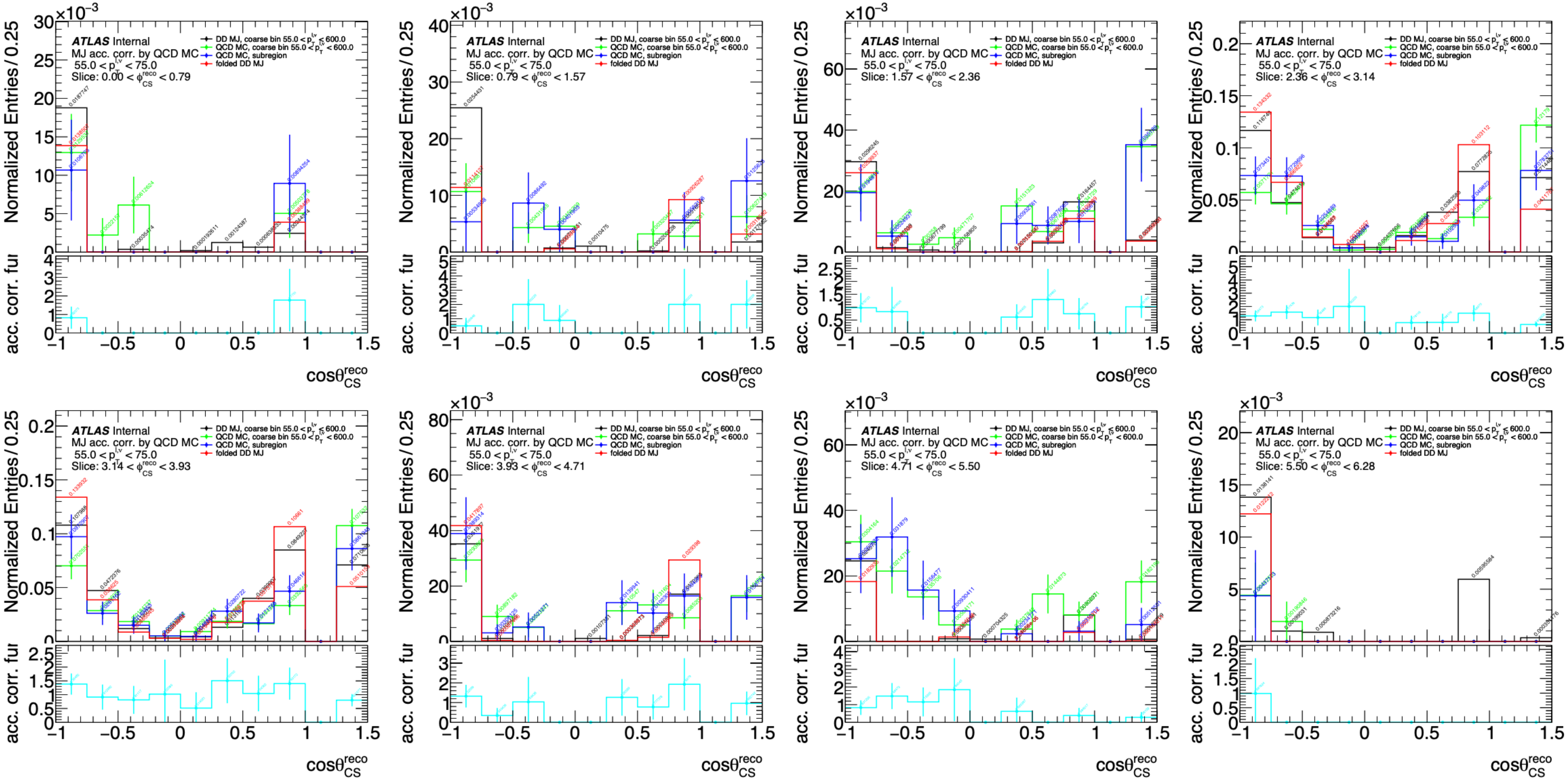

Figure 166: Multi-jet background template acceptance correction functions for $\cos\theta_{CS}$ as slices of ϕ_{CS} for $55 < p_T^{\ell,\nu} < 75$ GeV bin for $W^- \rightarrow e^-\bar{\nu}$ channel. Distributions are normalized over ϕ_{CS} slices. Error bands represents statistical uncertainties.

Acc Correction for 3D templates

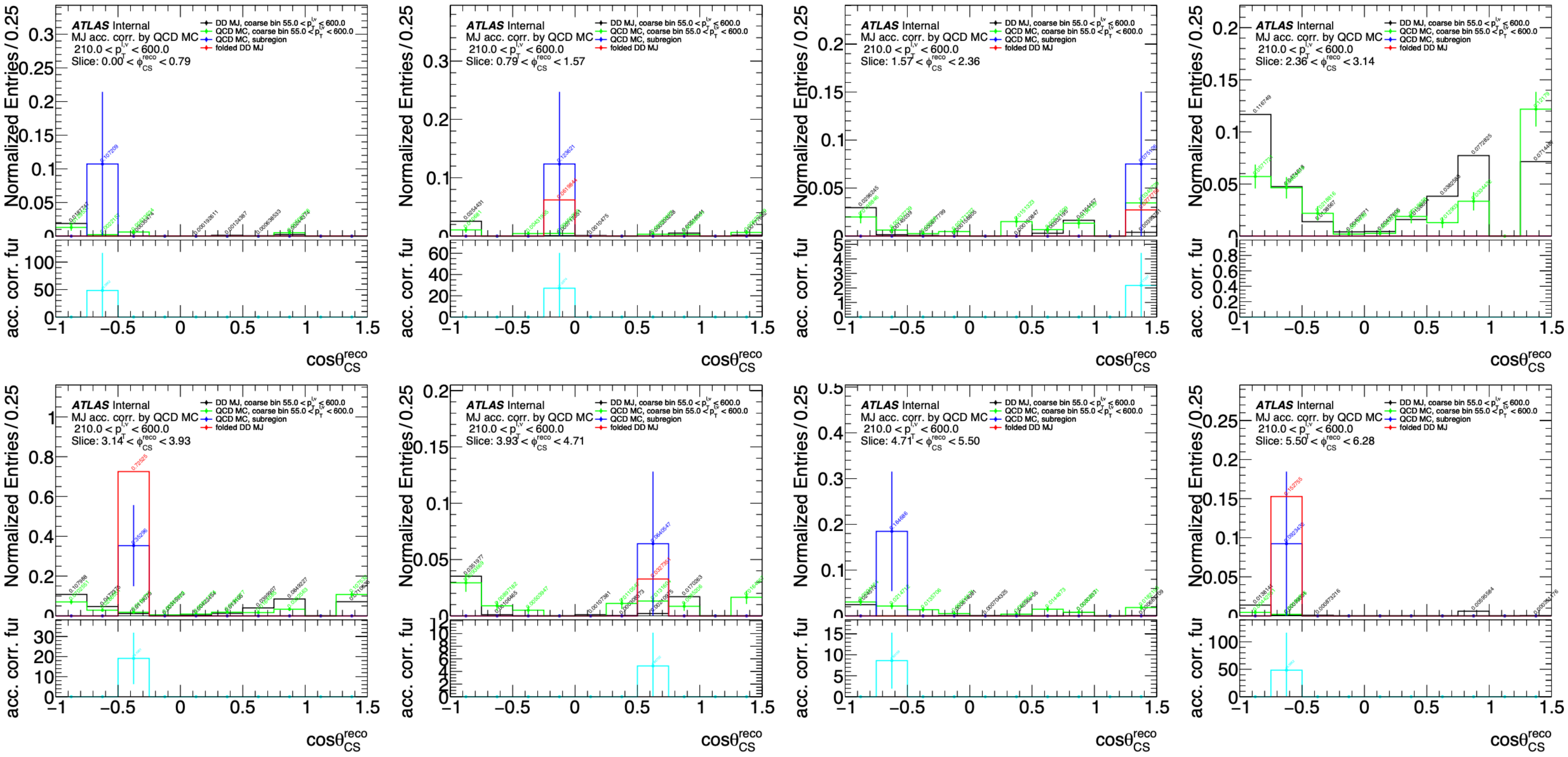

Figure 170: Multi-jet background template acceptance correction functions for $\cos\theta_{CS}$ as slices of ϕ_{CS} for $210 < p_T^{\ell,\nu} < 600$ GeV bin for $W^- \to e^-\overline{\nu}$ channel. Distributions are normalized over ϕ_{CS} slices. Error bands represents statistical uncertainties.